

The two loop supersymmetric corrections to lepton anomalous dipole moments in split supersymmetry scenarios

Tai-Fu Feng, Lin Sun, Xiu-Yi Yang

Department of Physics, Dalian University of Technology, Dalian, 116024, China

(Dated: December 4, 2018)

Abstract

An analysis of electroweak corrections to the anomalous dipole moments of lepton from some special two-loop diagrams where a closed neutralino/chargino loop is inserted into relevant one-loop diagrams of the standard model is presented in the split supersymmetry scenarios. Considering the translational invariance of the inner loop momenta and the electromagnetic gauge invariance, we get all dimension 6 operators and their coefficients. After applying equations of motion to the external leptons, we obtain the anomalous dipole moments of lepton. The numerical results imply that there is parameter space where the contribution to the muon anomalous magnetic dipole moment from this sector is perhaps significant, and the contribution to the electron electric dipole moment from this sector is sizable enough to be observed in next generation experiments.

PACS numbers: 11.30.Er, 12.60.Jv, 14.80.Cp

Keywords: magnetic and electric dipole moments, two-loop electroweak corrections, supersymmetry

I. INTRODUCTION

At both aspects of experiment and theory, the magnetic dipole moment (MDM) of lepton draws the great attention of physicists because of its obvious importance. The anomalous dipole moments of lepton not only can be used for testing loop effect in the standard model (SM), but also provide a potential window to detect new physics beyond the SM. The current experimental result of the muon MDM is [1]

$$a_{\mu}^{exp} = 11\,659\,208 \pm 6 \times 10^{-10}. \quad (1)$$

From the theoretical point of view, contributions to the muon MDM are generally divided into three sectors [2]: QED loops, hadronic contributions and electroweak corrections. With the hadronic contributions which are derived from the most recent e^+e^- data, we can get the following SM predictions [3, 4, 5]:

$$\begin{aligned} a_{\mu}^{SM} &= 11\,659\,180.9 \pm 8.0 \times 10^{-10}, \\ a_{\mu}^{SM} &= 11\,659\,175.6 \pm 7.5 \times 10^{-10}, \\ a_{\mu}^{SM} &= 11\,659\,179.4 \pm 9.3 \times 10^{-10}. \end{aligned} \quad (2)$$

The deviations between the above theoretical predictions and the experimental data are all approximately within error range of $\sim 2\sigma$. Although this $\sim 2\sigma$ deviation cannot be regarded as strong evidence for new physics, along with the experimental measurement precision and theoretical prediction accuracy being constantly improved, this deviation may become more significant in near future.

In fact, the current experimental precision (6×10^{-10}) already puts very restrictive bounds on new physics scenarios. In the SM, the electroweak one- and two-loop contributions amount to 19.5×10^{-10} and -4.4×10^{-10} [6] respectively. Comparing with the standard electroweak corrections, the electroweak corrections from new physics are generally suppressed by $\Lambda_{EW}^2/\Lambda_{NP}^2$, where Λ_{EW} denotes the electroweak energy scale and Λ_{NP} denotes the energy scale of new physics.

Supersymmetry (SUSY) has been considered a most prospective candidate for new physics beyond the SM. Nevertheless, the softly broken SUSY at electroweak scale induces many unwanted phenomenological problems, such as new sources of flavor changing neutral currents,

new CP violating phases etc. In order to solve those problems, the authors of literature [7] have recently proposed a split scenario. In this split scenario, SUSY is broken at a high energy scale that could be even near the scale of grand unification theory (GUT). A direct result of this assumption is that the scalar superpartners of SM fermions are all super heavy. On the other hand, charginos and neutralinos acquire masses around electroweak scale to TeV or so because of R-symmetry and PQ symmetry. Within this framework, heavy sfermions suppress the one-loop supersymmetric corrections to the processes of flavor changing neutral currents and lepton anomalous dipole moments at a negligible level. The leading contributions of new physics to theoretical predictions only arise from the two-loop diagrams in which a closed neutralino/chargino loop is inserted into relevant one loop SM diagrams, and the corresponding theoretical corrections are sizable enough to be well within the sensitivity of the next generation of experiments [8].

Actually, the two-loop electroweak corrections to the anomalous dipole moments of lepton are discussed extensively in literature. Utilizing the heavy mass expansion approximation (HME) together with the corresponding projection operator method, Ref.[9] has evaluated the two-loop standard electroweak corrections to the muon MDM. Within the framework of CP conservation, the authors of Ref. [10, 11] present the supersymmetric corrections from some special two-loop diagrams where a close chargino (neutralino) or scalar fermion loop is inserted into those two-Higgs-doublet one-loop diagrams. Ref. [12] discusses the contributions to the muon MDM from the effective vertices $H^\pm W^\mp \gamma$, $h_0(H_0)\gamma\gamma$ which are induced by the scalar quarks of the third generation in the minimal supersymmetric extension of SM. In the split scenario, the supersymmetric contributions to the electric dipole moment (EDM) of lepton have been already presented in Ref. [13, 14]. Under the assumption $|m_{1,2}|, |\mu_H| \gg m_w$,¹ the authors derive 5 CP-odd dimension 6 operators involving gauge fields and Higgs after they integrate out charginos and neutralinos at one-loop level. Inserting the effective couplings from those CP-odd dimension-6 operators into those relevant SM one-loop diagrams, they then get the lepton EDMs.

¹ m_2, m_1 denote the masses of $SU(2) \times U(1)$ gauginos in the soft breaking terms, and μ_H denotes the μ -parameter in the superpotential, respectively.

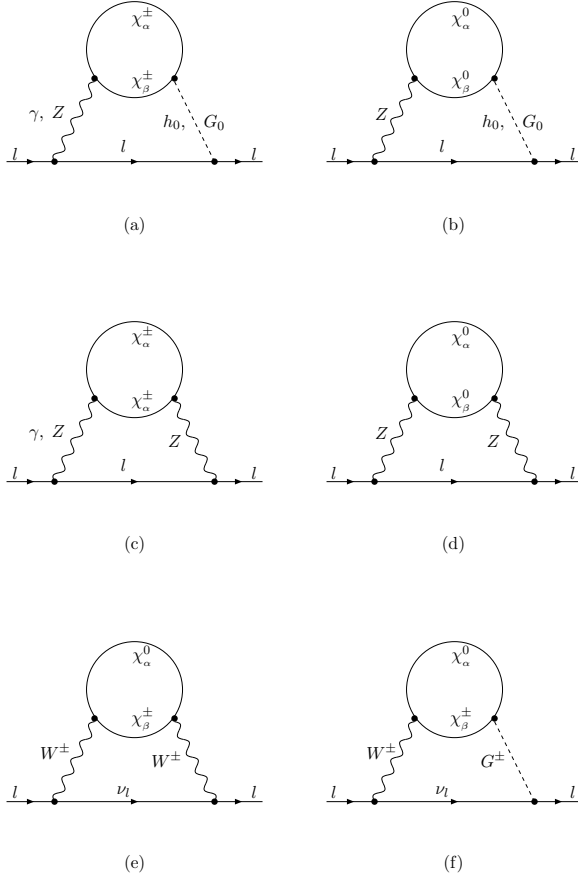


FIG. 1: The two-loop self energy diagrams which lead to the lepton MDMs and EDMs in split SUSY, the corresponding triangle diagrams are obtained by attaching a photon in all possible ways to the internal particles. In concrete calculation, the contributions from those mirror diagrams should be included also.

In this paper, we apply the effective Lagrangian method to get the anomalous dipole moments of lepton. The effective Lagrangian method has been adopted to calculate the two-loop supersymmetric corrections to the branching ratio of $b \rightarrow s\gamma$ [15], neutron EDM [16] and lepton MDMs and EDMs [17]. In concrete calculation, we assume that all external leptons as well as photon are off-shell, then expand the amplitude of corresponding triangle diagrams according to the external momenta of leptons and photon. Using loop momentum translational invariance, we formulate the sum of amplitude from those triangle diagrams

which correspond to the corresponding self-energy in the form which explicitly satisfies the Ward identity required by the QED gauge symmetry. Then we can get all dimension 6 operators together with their coefficients. After the equations of motion are applied to external leptons, higher dimensional operators, such as dimension 8 operators, also contribute to the muon MDM and the electron EDM in principle. However, the contributions of dimension 8 operators contain an additional suppression factor $m_l^2/\Lambda_{\text{NP}}^2$ comparing with that of dimension 6 operators, where m_l is the mass of lepton. Setting $\Lambda_{\text{NP}} \sim 100\text{GeV}$, one finds that this suppression factor is about 10^{-6} for muon, and 10^{-10} for electron separately. Under current experimental precision, it implies that the contributions of all higher dimension operators ($D \geq 8$) can be neglected safely.

We adopt the naive dimensional regularization with the anticommuting γ_5 scheme, where there is no distinction between the first 4 dimensions and the remaining $D - 4$ dimensions. Since the bare effective Lagrangian contains the ultraviolet divergence which is induced by divergent subdiagrams, we give the renormalized results in the on-mass-shell scheme [18]. Additional, we adopt the nonlinear R_ξ gauge with $\xi = 1$ for simplification [19]. This special gauge-fixing term guarantees explicit electromagnetic gauge invariance throughout the calculation, not just at the end because the choice of gauge-fixing term eliminates the $\gamma W^\pm G^\mp$ vertex in the Lagrangian.

Since the lepton EDM is an interesting topic in both theoretical and experimental aspects [20], the current experimental upper limit on the electron EDM is $1.7 \times 10^{-27} e \cdot \text{cm}$ at 95% CL[21], and a future experiment with precision of $10^{-29} e \cdot \text{cm}$ is also proposed[22], we as well present the lepton EDM by keeping all possible CP violating phases. Certainly, some diagrams in Fig.1 have been discussed in Ref.[11] where the authors apply the projecting operator to get the lepton MDMs (Eq.8~Eq.10 in Ref.[11]). Nevertheless, the substantive corrections from several diagrams are ignored unreasonably (Fig.5 in Ref.[11]). Additional, our formulae are new in their analytical forms. For the analysis on the electron EDM, we also include the contributions from the self energy diagrams (c) and (f) that are neglected in Ref.[13, 14]. Our result is more universal than that of Ref.[13, 14] because we give up the assumption $|m_{1,2}|, |\mu_H| \gg m_w$ in concrete analysis.

This paper is composed by the sections as follows. In section II, we introduce the effective

Lagrangian method and our notations. Then we will demonstrate how to obtain the supersymmetric two-loop corrections to the lepton MDMs and EDMs. Section III is devoted to the numerical analysis and discussion. In section IV, we give our conclusion. Some tedious formulae are collected in appendix.

II. NOTATIONS AND TWO-LOOP SUPERSYMMETRIC CORRECTIONS

The lepton MDMs and EDMs can actually be expressed as the operators

$$\begin{aligned}\mathcal{L}_{MDM} &= \frac{e}{4m_l} a_l \bar{l} \sigma^{\mu\nu} l F_{\mu\nu} , \\ \mathcal{L}_{EDM} &= -\frac{i}{2} d_l \bar{l} \sigma^{\mu\nu} \gamma_5 l F_{\mu\nu} .\end{aligned}\tag{3}$$

Here $\sigma_{\mu\nu} = i[\gamma_\mu, \gamma_\nu]/2$, l denotes the lepton fermion, $F_{\mu\nu}$ is the electromagnetic field strength, m_l is the lepton mass and e represents the electric charge. Note that the lepton here is on-shell.

In fact, it is convenient to get the corrections from loop diagrams to lepton MDMs and EDMs in terms of the effective Lagrangian method, if the masses of internal lines are much heavier than the external lepton mass. Assuming external leptons as well as photon are all off-shell, we expand the amplitude of the corresponding triangle diagrams according to the external momenta of leptons and photon. Then we can get all high dimension operators together with their coefficients. As discussed in the section I, it is enough to retain only those dimension 6 operators in later calculations:

$$\begin{aligned}\mathcal{O}_1^\mp &= \frac{1}{(4\pi)^2} \bar{l} (i\mathcal{D})^3 \omega_\mp l , \\ \mathcal{O}_2^\mp &= \frac{e}{(4\pi)^2} \overline{(i\mathcal{D}_\mu l)} \gamma^\mu F \cdot \sigma \omega_\mp l , \\ \mathcal{O}_3^\mp &= \frac{e}{(4\pi)^2} \bar{l} F \cdot \sigma \gamma^\mu \omega_\mp (i\mathcal{D}_\mu l) , \\ \mathcal{O}_4^\mp &= \frac{e}{(4\pi)^2} \bar{l} (\partial^\mu F_{\mu\nu}) \gamma^\nu \omega_\mp l , \\ \mathcal{O}_5^\mp &= \frac{m_l}{(4\pi)^2} \bar{l} (i\mathcal{D})^2 \omega_\mp l , \\ \mathcal{O}_6^\mp &= \frac{e Q_f m_l}{(4\pi)^2} \bar{l} F \cdot \sigma \omega_\mp l ,\end{aligned}\tag{4}$$

with $\mathcal{D}_\mu = \partial_\mu + ieA_\mu$ and $\omega_\mp = (1 \mp \gamma_5)/2$. When the equations of motion are applied to the incoming and outgoing leptons separately, only the operators $\mathcal{O}_{2,3,6}^\mp$ actually contribute to the MDMs and EDMs of leptons. We will only present the Wilson coefficients of the operators $\mathcal{O}_{2,3,6}^\mp$ in the effective Lagrangian in our following narration because of the reason mentioned above. We will adopt below a terminology where, for example, the " γh_0 " contribution means the sum of amplitude from those triangle diagrams (indeed three triangles bound together), in which a closed fermion (chargino/neutralino) loop is attached to the virtual Higgs and photon fields with a real photon attached in all possible ways to the internal lines. Because the sum of amplitude from those "triangle" diagrams corresponding to each "self-energy" obviously respects the Ward identity requested by QED gauge symmetry, we can calculate the contributions of all the "self-energies" separately. Taking the same steps which we did in our earlier works [15, 16, 17], we obtain the effective Lagrangian that originates from the self energy diagrams in Fig.1. In the bare effective Lagrangian from the 'WW' and 'ZZ' contributions, the ultraviolet divergence caused by divergent sub-diagrams can be subtracted safely in on-mass-shell scheme [18]. Now, we present the effective Lagrangian corresponding to the diagrams in Fig.1 respectively.

A. The effective Lagrangian from γh_0 (γG_0) sector

As a closed chargino loop is attached to the virtual neutral Higgs and photon fields, a real photon can be emitted from either the virtual lepton or the virtual charginos in the self energy diagram. When a real photon is emitted from the virtual charginos, the corresponding "triangle" diagrams belong to the typical two-loop Bar-Zee-type diagrams [23]. Within the framework of minimal supersymmetric extension of the SM, the contributions from two-loop Bar-Zee-type diagrams to the EDMs of those light fermions are discussed extensively in literature [24]. When a real photon is attached to the internal standard fermion, the correction from corresponding triangle diagram to the effective Lagrangian is zero because of the Furry theorem, this point is also verified through a strict analysis. The corresponding

effective Lagrangian from this sector is written as

$$\begin{aligned} \mathcal{L}_{\gamma h} = \frac{e^4}{2\sqrt{2}(4\pi)^2 s_w^2 \Lambda^2} & \left\{ \Re(\mathcal{H}_{\alpha\alpha}) \left(\frac{x_{x_\alpha^\pm}}{x_w} \right)^{1/2} T_1(x_h, x_{x_\alpha^\pm}, x_{x_\alpha^\pm}) (\mathcal{O}_6^+ + \mathcal{O}_6^-) \right. \\ & \left. + i\Im(\mathcal{H}_{\alpha\alpha}) \left(\frac{x_{x_\alpha^\pm}}{x_w} \right)^{1/2} T_2(x_h, x_{x_\alpha^\pm}, x_{x_\alpha^\pm}) (\mathcal{O}_6^+ - \mathcal{O}_6^-) \right\} \end{aligned} \quad (5)$$

with

$$\mathcal{H}_{\alpha\beta} = (U_R^\dagger)_{\alpha 2} (U_L)_{1\beta} \cos \beta + (U_R^\dagger)_{\alpha 1} (U_L)_{2\beta} \sin \beta. \quad (6)$$

Where $U_{L,R}$ denote the left- and right-mixing matrices of charginos, Λ denotes a energy scale to define $x_i = m_i^2/\Lambda^2$, respectively. The angle β is defined through the ratio between the vacuum expectation values of two Higgs doublets: $\tan \beta = v_2/v_1$. We adopt the shortcut notations: $c_w = \cos \theta_w$, $s_w = \sin \theta_w$, where θ_w is the Weinberg angle. The concrete expressions of $T_{1,2}$ can be found in appendix.

Accordingly, the lepton MDMs and EDMs from γh_0 sector are written as

$$\begin{aligned} a_l^{\gamma h} &= \frac{\sqrt{2}e^4 Q_f m_l^2}{(4\pi)^4 s_w^2 \Lambda^2} \Re(\mathcal{H}_{\alpha\alpha}) \left(\frac{x_{x_\alpha^\pm}}{x_w} \right)^{1/2} T_1(x_h, x_{x_\alpha^\pm}, x_{x_\alpha^\pm}), \\ d_l^{\gamma h} &= -\frac{e^5 Q_f m_l}{\sqrt{2}(4\pi)^4 s_w^2 \Lambda^2} \Im(\mathcal{H}_{\alpha\alpha}) \left(\frac{x_{x_\alpha^\pm}}{x_w} \right)^{1/2} T_2(x_h, x_{x_\alpha^\pm}, x_{x_\alpha^\pm}). \end{aligned} \quad (7)$$

In the limit $x_{x_\alpha^\pm} \gg x_h$, the above expressions can be simplified as

$$\begin{aligned} a_l^{\gamma h} &= -\frac{\sqrt{2}e^4 Q_f m_l^2}{(4\pi)^4 s_w^2 \Lambda^2} \Re(\mathcal{H}_{\alpha\alpha}) \left(\frac{x_{x_\alpha^\pm}}{x_w} \right)^{1/2} \lim_{x_{x_\beta^\pm} \rightarrow x_{x_\alpha^\pm}} \frac{\partial}{\partial x_{x_\beta^\pm}} \varphi_1(x_{x_\alpha^\pm}, x_{x_\beta^\pm}), \\ d_l^{\gamma h} &= -\frac{e^5 Q_f m_l}{\sqrt{2}(4\pi)^4 s_w^2 \Lambda^2} \Im(\mathcal{H}_{\alpha\alpha}) \left(\frac{x_{x_\alpha^\pm}}{x_w} \right)^{1/2} \left[\frac{\ln x_h}{x_{x_\alpha^\pm}} + \lim_{x_{x_\beta^\pm} \rightarrow x_{x_\alpha^\pm}} \frac{\partial}{\partial x_{x_\beta^\pm}} \varphi_1(x_{x_\alpha^\pm}, x_{x_\beta^\pm}) \right]. \end{aligned} \quad (8)$$

Similarly, we can formulate the corrections from γG_0 sector to the effective Lagrangian as

$$\begin{aligned} \mathcal{L}_{\gamma G} = \frac{e^4}{2\sqrt{2}(4\pi)^2 s_w^2 \Lambda^2} & \left\{ \Re(\mathcal{H}_{\alpha\alpha}) \left(\frac{x_{x_\alpha^\pm}}{x_w} \right)^{1/2} T_2(x_z, x_{x_\alpha^\pm}, x_{x_\beta^\pm}) \right. \\ & \left. - i\Im(\mathcal{H}_{\alpha\alpha}) \left(\frac{x_{x_\alpha^\pm}}{x_w} \right)^{1/2} T_1(x_z, x_{x_\alpha^\pm}, x_{x_\beta^\pm}) (\mathcal{O}_6^+ - \mathcal{O}_6^-) \right\}. \end{aligned} \quad (9)$$

Correspondingly, the corrections to the lepton MDMs and EDMs from this sector are:

$$\begin{aligned}
a_l^{\gamma G} &= \frac{\sqrt{2}e^4 Q_f m_l^2}{(4\pi)^4 s_w^2 \Lambda^2} \Re(\mathcal{H}_{\alpha\alpha}) \left(\frac{x_{x_\alpha^\pm}}{x_w}\right)^{1/2} T_2(x_z, x_{x_\alpha^\pm}, x_{x_\alpha^\pm}), \\
d_l^{\gamma G} &= \frac{e^5 Q_f m_l}{\sqrt{2}(4\pi)^4 s_w^2 \Lambda^2} \Im(\mathcal{H}_{\alpha\alpha}) \left(\frac{x_{x_\alpha^\pm}}{x_w}\right)^{1/2} T_1(x_z, x_{x_\alpha^\pm}, x_{x_\alpha^\pm}).
\end{aligned} \tag{10}$$

In the limit $x_{x_\alpha^\pm} \gg x_z$, we have

$$\begin{aligned}
a_l^{\gamma G} &= \frac{\sqrt{2}e^4 Q_f m_l^2}{(4\pi)^4 s_w^2 \Lambda^2} \Re(\mathcal{H}_{\alpha\alpha}) \left(\frac{x_{x_\alpha^\pm}}{x_w}\right)^{1/2} \left[\frac{\ln x_z}{x_{x_\alpha^\pm}} + \lim_{x_{x_\beta^\pm} \rightarrow x_{x_\alpha^\pm}} \frac{\partial}{\partial x_{x_\beta^\pm}} \varphi_1(x_{x_\alpha^\pm}, x_{x_\beta^\pm}) \right], \\
d_l^{\gamma G} &= \frac{e^5 Q_f m_l}{\sqrt{2}(4\pi)^4 s_w^2 \Lambda^2} \Im(\mathcal{H}_{\alpha\alpha}) \left(\frac{x_{x_\alpha^\pm}}{x_w}\right)^{1/2} \lim_{x_{x_\beta^\pm} \rightarrow x_{x_\alpha^\pm}} \frac{\partial}{\partial x_{x_\beta^\pm}} \varphi_1(x_{x_\alpha^\pm}, x_{x_\beta^\pm}).
\end{aligned} \tag{11}$$

It should be emphasized that the corrections from this sector to the lepton EDMs are neglected in the analysis before [13, 14]. However, Eq.10 implies that the contributions from those diagrams to the lepton MDMs and EDMs can not be ignored generally.

Using the concrete expression of $\varphi_1(x, y)$ collected in appendix, one can verify easily that the corrections to the lepton MDMs and EDMs from the sectors are suppressed by the masses of charginos as $m_{x_\alpha^\pm} \gg m_h, m_z$ ($\alpha = 1, 2$).

B. The effective Lagrangian from Zh_0 (ZG_0) sector

As a closed chargino loop is attached to the virtual Higgs and Z gauge boson fields, a real photon can be attached to either the virtual lepton or the virtual charginos in the self energy diagram. When a real photon is attached to the virtual lepton, the corresponding amplitude only modifies the Wilson coefficients of the operators \mathcal{O}_5^\pm in the effective Lagrangian after the heavy freedoms are integrated out. In other words, this triangle diagram does not contribute to the lepton MDMs and EDMs. A real photon can be only attached to the virtual lepton as the closed loop is composed of neutralinos, the corresponding triangle diagram does not affect the theoretical predictions on the lepton MDMs and EDMs for the same reason. Considering the points above, we formulate the contributions from Zh_0 sector to the effective Lagrangian as

$$\mathcal{L}_{zh} = -\frac{e^4}{16\sqrt{2}(4\pi)^2 s_w^4 c_w^2 Q_f \Lambda^2} (T_f^Z - 2Q_f s_w^2) \left\{ \left(\frac{x_{x_\beta^\pm}}{x_w}\right)^{1/2} \left[2(2 + \ln x_{x_\beta^\pm}) \varrho_{0,1}(x_z, x_h) \right] \right.$$

$$\begin{aligned}
& +F_1(x_z, x_h, x_{\chi_\alpha^\pm}, x_{\chi_\beta^\pm}) \Big] \Re(\mathcal{H}_{\beta\alpha} \xi_{\alpha\beta}^L + \mathcal{H}_{\beta\alpha}^\dagger \xi_{\alpha\beta}^R)(\mathcal{O}_6^+ + \mathcal{O}_6^-) \\
& +i\left(\frac{x_{\chi_\beta^\pm}}{x_w}\right)^{1/2} \left[-2(\ln x_{\chi_\alpha^\pm} - \ln x_{\chi_\beta^\pm}) \varrho_{0,1}(x_z, x_h) + F_1(x_z, x_h, x_{\chi_\alpha^\pm}, x_{\chi_\beta^\pm}) \right. \\
& \left. +F_2(x_z, x_h, x_{\chi_\beta^\pm}, x_{\chi_\alpha^\pm}) \right] \Im(\mathcal{H}_{\beta\alpha} \xi_{\alpha\beta}^L - \mathcal{H}_{\beta\alpha}^\dagger \xi_{\alpha\beta}^R)(\mathcal{O}_6^- - \mathcal{O}_6^+) \Big\} + \dots \tag{12}
\end{aligned}$$

with

$$\begin{aligned}
\xi_{\alpha\beta}^L &= 2\delta_{\alpha\beta} \cos 2\theta_w + (U_L^\dagger)_{\alpha 1} (U_L)_{1\beta} , \\
\xi_{\alpha\beta}^R &= 2\delta_{\alpha\beta} \cos 2\theta_w + (U_R^\dagger)_{\alpha 1} (U_R)_{1\beta} , \tag{13}
\end{aligned}$$

where the concrete expressions of the functions $\varrho_{i,j}(x_1, x_2)$, $F_{1,2}(x_1, x_2, x_3, x_4)$ are listed in appendix. Additional, T_f^Z is the isospin of lepton, and Q_f is the electric charge of lepton, respectively. Using Eq.12, we get the corrections to the lepton MDMs and EDMs from Zh_0 sector as

$$\begin{aligned}
a_l^{Zh} &= -\frac{e^4 m_l^2}{4\sqrt{2}(4\pi)^4 s_w^4 c_w^2 \Lambda^2} (T_f^Z - 2Q_f s_w^2) \left(\frac{x_{\chi_\beta^\pm}}{x_w}\right)^{1/2} \left[2(2 + \ln x_{\chi_\beta^\pm}) \varrho_{i,j}(x_z, x_h) \right. \\
& \left. +F_1(x_z, x_h, x_{\chi_\alpha^\pm}, x_{\chi_\beta^\pm}) \right] \Re(\mathcal{H}_{\beta\alpha} \xi_{\alpha\beta}^L + \mathcal{H}_{\beta\alpha}^\dagger \xi_{\alpha\beta}^R) , \\
d_l^{Zh} &= \frac{e^5 m_l}{8\sqrt{2}(4\pi)^4 s_w^4 c_w^2 \Lambda^2} (T_f^Z - 2Q_f s_w^2) \left(\frac{x_{\chi_\beta^\pm}}{x_w}\right)^{1/2} \left[-2(\ln x_{\chi_\alpha^\pm} - \ln x_{\chi_\beta^\pm}) \varrho_{0,1}(x_z, x_h) \right. \\
& \left. +F_1(x_z, x_h, x_{\chi_\alpha^\pm}, x_{\chi_\beta^\pm}) + F_2(x_z, x_h, x_{\chi_\beta^\pm}, x_{\chi_\alpha^\pm}) \right] \Im(\mathcal{H}_{\beta\alpha} \xi_{\alpha\beta}^L - \mathcal{H}_{\beta\alpha}^\dagger \xi_{\alpha\beta}^R) . \tag{14}
\end{aligned}$$

The above equations contain the suppression factor $1-4s_w^2$ because $Q_f = -1$ and $T_f^Z = -1/2$ for charged leptons. In the limit $x_{\chi_\alpha^\pm}, x_{\chi_\beta^\pm} \gg x_z, x_h$, Eq.14 can be approximated as

$$\begin{aligned}
a_l^{Zh} &= -\frac{e^4 m_l^2}{4\sqrt{2}(4\pi)^4 s_w^4 c_w^2 \Lambda^2} (T_f^Z - 2Q_f s_w^2) \left(\frac{x_{\chi_\beta^\pm}}{x_w}\right)^{1/2} \left[\frac{\partial \varphi_1}{\partial x_{\chi_\beta^\pm}}(x_{\chi_\alpha^\pm}, x_{\chi_\beta^\pm}) \right. \\
& \left. - \frac{2 - 2x_{\chi_\alpha^\pm} \varrho_{0,1}(x_{\chi_\alpha^\pm}, x_{\chi_\beta^\pm})}{x_{\chi_\alpha^\pm} - x_{\chi_\beta^\pm}} \cdot \varrho_{1,1}(x_z, x_h) \right] \Re(\mathcal{H}_{\beta\alpha} \xi_{\alpha\beta}^L + \mathcal{H}_{\beta\alpha}^\dagger \xi_{\alpha\beta}^R) , \\
d_l^{Zh} &= \frac{e^5 m_l}{8\sqrt{2}(4\pi)^4 s_w^4 c_w^2 \Lambda^2} (T_f^Z - 2Q_f s_w^2) \left(\frac{x_{\chi_\beta^\pm}}{x_w}\right)^{1/2} \left[\left(\frac{\partial \varphi_1}{\partial x_{\chi_\alpha^\pm}} + \frac{\partial \varphi_1}{\partial x_{\chi_\beta^\pm}} \right) (x_{\chi_\alpha^\pm}, x_{\chi_\beta^\pm}) \right. \\
& \left. + 2\varrho_{0,1}(x_{\chi_\alpha^\pm}, x_{\chi_\beta^\pm}) \varrho_{1,1}(x_z, x_h) \right] \Im(\mathcal{H}_{\beta\alpha} \xi_{\alpha\beta}^L - \mathcal{H}_{\beta\alpha}^\dagger \xi_{\alpha\beta}^R) . \tag{15}
\end{aligned}$$

Similarly, the contributions from ZG_0 sector to the effective Lagrangian are

$$\begin{aligned}
\mathcal{L}_{ZG_0} = & -\frac{e^4}{16\sqrt{2}(4\pi)^2 s_w^4 c_w^2 Q_f \Lambda^2} \left\{ -i \left(\frac{x_{x_\beta^\pm}}{x_w} \right)^{1/2} \left[\frac{2}{x_z} (2 + \ln x_{x_\beta^\pm}) + F_1(x_z, x_z, x_{x_\alpha^\pm}, x_{x_\beta^\pm}) \right] \right. \\
& \times \Im \left(\mathcal{H}_{\beta\alpha} \xi_{\alpha\beta}^L + \mathcal{H}_{\beta\alpha}^\dagger \xi_{\alpha\beta}^R \right) (T_f^Z - 2Q_f s_w^2) (\mathcal{O}_6^- - \mathcal{O}_6^+) \\
& + \left(\frac{x_{x_\beta^\pm}}{x_w} \right)^{1/2} \left[-\frac{2}{x_z} (\ln x_{x_\alpha^\pm} - \ln x_{x_\beta^\pm}) + F_1(x_z, x_z, x_{x_\alpha^\pm}, x_{x_\beta^\pm}) + F_2(x_z, x_z, x_{x_\beta^\pm}, x_{x_\alpha^\pm}) \right] \\
& \left. \times \Re \left(\mathcal{H}_{\beta\alpha} \xi_{\alpha\beta}^L - \mathcal{H}_{\beta\alpha}^\dagger \xi_{\alpha\beta}^R \right) (T_f^Z - 2Q_f s_w^2) (\mathcal{O}_6^- + \mathcal{O}_6^+) \right\} + \dots, \tag{16}
\end{aligned}$$

and the contributions to the lepton MDMs and EDMs are:

$$\begin{aligned}
a_l^{ZG} = & -\frac{e^4 m_l^2}{4\sqrt{2}(4\pi)^4 s_w^4 c_w^2 \Lambda^2} (T_f^Z - 2Q_f s_w^2) \left(\frac{x_{x_\beta^\pm}}{x_w} \right)^{1/2} \left[-\frac{2}{x_z} (\ln x_{x_\alpha^\pm} - \ln x_{x_\beta^\pm}) \right. \\
& \left. + F_1(x_z, x_z, x_{x_\alpha^\pm}, x_{x_\beta^\pm}) + F_2(x_z, x_z, x_{x_\beta^\pm}, x_{x_\alpha^\pm}) \right] \Re \left(\mathcal{H}_{\beta\alpha} \xi_{\alpha\beta}^L - \mathcal{H}_{\beta\alpha}^\dagger \xi_{\alpha\beta}^R \right), \\
d_l^{ZG} = & \frac{e^5 m_l}{8\sqrt{2}(4\pi)^4 s_w^4 c_w^2 \Lambda^2} (T_f^Z - 2Q_f s_w^2) \left(\frac{x_{x_\beta^\pm}}{x_w} \right)^{1/2} \left[\frac{2}{x_z} (2 + \ln x_{x_\beta^\pm}) \right. \\
& \left. + F_1(x_z, x_z, x_{x_\alpha^\pm}, x_{x_\beta^\pm}) \right] \Im \left(\mathcal{H}_{\beta\alpha} \xi_{\alpha\beta}^L + \mathcal{H}_{\beta\alpha}^\dagger \xi_{\alpha\beta}^R \right). \tag{17}
\end{aligned}$$

When $x_{x_\alpha^\pm}, x_{x_\beta^\pm} \gg x_z$, Eq.17 can be approached by

$$\begin{aligned}
a_l^{ZG} = & -\frac{e^4 m_l^2}{4\sqrt{2}(4\pi)^4 s_w^4 c_w^2 \Lambda^2} (T_f^Z - 2Q_f s_w^2) \left(\frac{x_{x_\beta^\pm}}{x_w} \right)^{1/2} \left[\left(\frac{\partial \varphi_1}{\partial x_{x_\alpha^\pm}} + \frac{\partial \varphi_1}{\partial x_{x_\beta^\pm}} \right) (x_{x_\alpha^\pm}, x_{x_\beta^\pm}) \right. \\
& \left. + 2(1 + \ln x_z) \varrho_{0,1}(x_{x_\alpha^\pm}, x_{x_\beta^\pm}) \right] \Re \left(\mathcal{H}_{\beta\alpha} \xi_{\alpha\beta}^L - \mathcal{H}_{\beta\alpha}^\dagger \xi_{\alpha\beta}^R \right), \\
d_l^{ZG} = & \frac{e^5 m_l}{8\sqrt{2}(4\pi)^4 s_w^4 c_w^2 \Lambda^2} (T_f^Z - 2Q_f s_w^2) \left(\frac{x_{x_\beta^\pm}}{x_w} \right)^{1/2} \left[\frac{\partial \varphi_1}{\partial x_{x_\beta^\pm}} (x_{x_\alpha^\pm}, x_{x_\beta^\pm}) \right. \\
& \left. - \frac{2 - 2x_{x_\alpha^\pm} \varrho_{0,1}(x_{x_\alpha^\pm}, x_{x_\beta^\pm})}{x_{x_\alpha^\pm} - x_{x_\beta^\pm}} \cdot (1 + \ln x_z) \right] \Im \left(\mathcal{H}_{\beta\alpha} \xi_{\alpha\beta}^L + \mathcal{H}_{\beta\alpha}^\dagger \xi_{\alpha\beta}^R \right). \tag{18}
\end{aligned}$$

C. The effective Lagrangian from γZ sector

When a closed chargino loop is attached to the virtual γ and Z gauge bosons, the corresponding correction to the effective Lagrangian is very tedious. If we ignore the terms which are proportional to the suppression factor $1 - 4s_w^2$, the correction from this sector to

the effective Lagrangian is drastically simplified as

$$\begin{aligned} \mathcal{L}_{\gamma Z} = & \frac{e^4}{8(4\pi)^2 s_w^2 c_w^2 \Lambda^2} (\xi_{\alpha\alpha}^L - \xi_{\alpha\alpha}^R) \lim_{x_{\chi_\alpha^\pm} \rightarrow x_{\chi_\beta^\pm}} T_3(x_z, x_{\chi_\alpha^\pm}, x_{\chi_\beta^\pm}) \\ & \times \left[(T_f^Z - Q_f s_w^2) (\mathcal{O}_2^- + \mathcal{O}_3^-) + Q_f s_w^2 (\mathcal{O}_2^+ + \mathcal{O}_3^+) \right] + \dots \end{aligned} \quad (19)$$

Correspondingly, the correction to the lepton MDMs from this sector is written as

$$a_l^{\gamma Z} = \frac{e^4 m_l^2}{4(4\pi)^4 s_w^2 c_w^2 \Lambda^2} (\xi_{\alpha\alpha}^L - \xi_{\alpha\alpha}^R) \lim_{x_{\chi_\beta^\pm} \rightarrow x_{\chi_\alpha^\pm}} T_3(x_z, x_{\chi_\alpha^\pm}, x_{\chi_\beta^\pm}), \quad (20)$$

and the correction to the lepton EDMs is zero. In the limit $x_{\chi_\alpha^\pm} \gg x_z$, we can approximate the correction to the lepton MDMs from this sector as

$$\begin{aligned} a_l^{\gamma Z} = & \frac{e^4 m_l^2}{4(4\pi)^4 s_w^2 c_w^2 \Lambda^2} (\xi_{\alpha\alpha}^L - \xi_{\alpha\alpha}^R) \left[\frac{13}{18x_{\chi_\alpha^\pm}} + \frac{\ln x_{\chi_\alpha^\pm} - 2 \ln x_z}{3x_{\chi_\alpha^\pm}} \right. \\ & \left. + \lim_{x_{\chi_\beta^\pm} \rightarrow x_{\chi_\alpha^\pm}} \left(2x_{\chi_\alpha^\pm} \frac{\partial^2 \varphi_1}{\partial x^2} - \frac{\partial \varphi_1}{\partial x} \right) (x_{\chi_\alpha^\pm}, x_{\chi_\beta^\pm}) \right]. \end{aligned} \quad (21)$$

D. The effective Lagrangian from WG^\pm sector

As a closed chargino-neutralino loop is attached to the virtual W^\pm gauge boson and charged goldstone G^\mp , the induced Lagrangian can be written as

$$\begin{aligned} \mathcal{L}_{WG} = & \frac{e^4}{16(4\pi)^2 s_w^4 c_w Q_f \Lambda^2} \left\{ \left(\frac{x_{\chi_\beta^\pm}}{x_w} \right)^{1/2} F_3(x_w, x_w, x_{\chi_\alpha^0}, x_{\chi_\beta^\pm}) \left[(\mathcal{G}_{\beta\alpha}^L \zeta_{\alpha\beta}^L + \mathcal{G}_{\beta\alpha}^R \zeta_{\alpha\beta}^R) \mathcal{O}_6^- \right. \right. \\ & \left. \left. + ((\mathcal{G}_{\alpha\beta}^L)^\dagger (\zeta_{\beta\alpha}^L)^\dagger + (\mathcal{G}_{\alpha\beta}^R)^\dagger (\zeta_{\beta\alpha}^R)^\dagger) \mathcal{O}_6^+ \right] \right. \\ & \left. + \left(\frac{x_{\chi_\alpha^0}}{x_w} \right)^{1/2} F_4(x_w, x_w, x_{\chi_\alpha^0}, x_{\chi_\beta^\pm}) \left[(\mathcal{G}_{\beta\alpha}^L \zeta_{\alpha\beta}^R + \mathcal{G}_{\beta\alpha}^R \zeta_{\alpha\beta}^L) \mathcal{O}_6^- + ((\mathcal{G}_{\alpha\beta}^R)^\dagger (\zeta_{\beta\alpha}^L)^\dagger \right. \right. \\ & \left. \left. + (\mathcal{G}_{\alpha\beta}^L)^\dagger (\zeta_{\beta\alpha}^R)^\dagger) \mathcal{O}_6^+ \right] \right. \\ & \left. + \left(\frac{x_{\chi_\beta^\pm}}{x_w} \right)^{1/2} F_5(x_w, x_w, x_{\chi_\alpha^0}, x_{\chi_\beta^\pm}) \left[(\mathcal{G}_{\beta\alpha}^L \zeta_{\alpha\beta}^L - \mathcal{G}_{\beta\alpha}^R \zeta_{\alpha\beta}^R) \mathcal{O}_6^- + ((\mathcal{G}_{\alpha\beta}^L)^\dagger (\zeta_{\beta\alpha}^L)^\dagger \right. \right. \\ & \left. \left. - (\mathcal{G}_{\alpha\beta}^R)^\dagger (\zeta_{\beta\alpha}^R)^\dagger) \mathcal{O}_6^+ \right] \right. \\ & \left. + \left(\frac{x_{\chi_\alpha^0}}{x_w} \right)^{1/2} F_6(x_w, x_w, x_{\chi_\alpha^0}, x_{\chi_\beta^\pm}) \left[(\mathcal{G}_{\beta\alpha}^L \zeta_{\alpha\beta}^R - \mathcal{G}_{\beta\alpha}^R \zeta_{\alpha\beta}^L) \mathcal{O}_6^- + ((\mathcal{G}_{\alpha\beta}^L)^\dagger (\zeta_{\beta\alpha}^R)^\dagger \right. \right. \\ & \left. \left. - (\mathcal{G}_{\alpha\beta}^R)^\dagger (\zeta_{\beta\alpha}^L)^\dagger) \mathcal{O}_6^+ \right] \right\} \end{aligned} \quad (22)$$

with

$$\begin{aligned}
\zeta_{\alpha\beta}^L &= \mathcal{N}_{\alpha 2}^\dagger (U_R)_{1\beta} - \frac{1}{\sqrt{2}} \mathcal{N}_{\alpha 4}^\dagger (U_R)_{2\beta} , \\
\zeta_{\alpha\beta}^R &= \mathcal{N}_{2\alpha} (U_R^\dagger)_{\beta 1} + \frac{1}{\sqrt{2}} \mathcal{N}_{3\alpha} (U_R^\dagger)_{\beta 2} , \\
\mathcal{G}_{\beta\alpha}^L &= \sin \beta \left\{ \frac{1}{\sqrt{2}} (U_L)_{2\beta} (\mathcal{N}_{1\alpha} s_w + \mathcal{N}_{2\alpha} c_w) - (U_L)_{1\beta} \mathcal{N}_{3\alpha} c_w \right\} , \\
\mathcal{G}_{\beta\alpha}^R &= -\cos \beta \left\{ \frac{1}{\sqrt{2}} (U_R^\dagger)_{\beta 2} (\mathcal{N}_{\alpha 1} s_w + \mathcal{N}_{\alpha 2} c_w) - (U_R^\dagger)_{\beta 1} \mathcal{N}_{\alpha 4} c_w \right\} .
\end{aligned} \tag{23}$$

Here, the 4×4 matrix \mathcal{N} denotes the mixing matrix of the four neutralinos χ_α^0 ($\alpha = 1, 2, 3, 4$).

The corresponding corrections to the lepton MDMs and EDMs are respectively expressed as

$$\begin{aligned}
a_l^{WG} &= \frac{e^4 m_l^2}{4(4\pi)^4 s_w^4 c_w \Lambda^2} \left\{ \left(\frac{x_{\chi_\beta^\pm}}{x_w} \right)^{1/2} F_3(x_w, x_w, x_{\chi_\alpha^0}, x_{\chi_\beta^\pm}) \Re(\mathcal{G}_{\beta\alpha}^L \zeta_{\alpha\beta}^L + \mathcal{G}_{\beta\alpha}^R \zeta_{\alpha\beta}^R) \right. \\
&\quad + \left(\frac{x_{\chi_\alpha^0}}{x_w} \right)^{1/2} F_4(x_w, x_w, x_{\chi_\alpha^0}, x_{\chi_\beta^\pm}) \Re(\mathcal{G}_{\beta\alpha}^L \zeta_{\alpha\beta}^R + \mathcal{G}_{\beta\alpha}^R \zeta_{\alpha\beta}^L) \\
&\quad + \left(\frac{x_{\chi_\beta^\pm}}{x_w} \right)^{1/2} F_5(x_w, x_w, x_{\chi_\alpha^0}, x_{\chi_\beta^\pm}) \Re(\mathcal{G}_{\beta\alpha}^L \zeta_{\alpha\beta}^L - \mathcal{G}_{\beta\alpha}^R \zeta_{\alpha\beta}^R) \\
&\quad \left. + \left(\frac{x_{\chi_\alpha^0}}{x_w} \right)^{1/2} F_6(x_w, x_w, x_{\chi_\alpha^0}, x_{\chi_\beta^\pm}) \Re(\mathcal{G}_{\beta\alpha}^L \zeta_{\alpha\beta}^R - \mathcal{G}_{\beta\alpha}^R \zeta_{\alpha\beta}^L) \right\} , \\
d_l^{WG} &= \frac{e^5 m_l}{8(4\pi)^4 s_w^4 c_w \Lambda^2} \left\{ \left(\frac{x_{\chi_\beta^\pm}}{x_w} \right)^{1/2} F_3(x_w, x_w, x_{\chi_\alpha^0}, x_{\chi_\beta^\pm}) \Im(\mathcal{G}_{\beta\alpha}^L \zeta_{\alpha\beta}^L + \mathcal{G}_{\beta\alpha}^R \zeta_{\alpha\beta}^R) \right. \\
&\quad + \left(\frac{x_{\chi_\alpha^0}}{x_w} \right)^{1/2} F_4(x_w, x_w, x_{\chi_\alpha^0}, x_{\chi_\beta^\pm}) \Im(\mathcal{G}_{\beta\alpha}^L \zeta_{\alpha\beta}^R + \mathcal{G}_{\beta\alpha}^R \zeta_{\alpha\beta}^L) \\
&\quad + \left(\frac{x_{\chi_\beta^\pm}}{x_w} \right)^{1/2} F_5(x_w, x_w, x_{\chi_\alpha^0}, x_{\chi_\beta^\pm}) \Im(\mathcal{G}_{\beta\alpha}^L \zeta_{\alpha\beta}^L - \mathcal{G}_{\beta\alpha}^R \zeta_{\alpha\beta}^R) \\
&\quad \left. + \left(\frac{x_{\chi_\alpha^0}}{x_w} \right)^{1/2} F_6(x_w, x_w, x_{\chi_\alpha^0}, x_{\chi_\beta^\pm}) \Im(\mathcal{G}_{\beta\alpha}^L \zeta_{\alpha\beta}^R - \mathcal{G}_{\beta\alpha}^R \zeta_{\alpha\beta}^L) \right\} .
\end{aligned} \tag{24}$$

Using the asymptotic formulations of form factors $T_{4,5,6,7}$ collected in appendix, we can simplify the expressions of Eq.24 in the limit $x_{\chi_\alpha^0}, x_{\chi_\beta^\pm} \gg x_w$.

The contributions from those above sectors to effective Lagrangian do not contain ultraviolet divergence. In the pieces discussed below, the coefficients of high dimensional operators in effective Lagrangian contain ultraviolet divergence that is caused by the divergent subdiagrams. In order to obtain physical predictions of lepton MDMs and EDMs,

it is necessary to adopt a concrete renormalization scheme removing the ultraviolet divergence. In literature, the on-shell renormalization scheme is adopted frequently to subtract the ultraviolet divergence which appears in the radiative electroweak corrections [18]. As an over-subtract scheme, the counter terms include some finite terms which originate from those renormalization conditions in the on-shell scheme beside the ultraviolet divergence to cancel the corresponding ultraviolet divergence in the bare Lagrangian. In the concrete calculation performed here, we apply this scheme to subtract the ultraviolet divergence caused by the divergent subdiagrams.

E. The effective Lagrangian from the ZZ sector

The self energy of Z gauge boson composed of a closed chargino loop induces the ultraviolet divergence in the Wilson coefficients of effective Lagrangian. Generally, the unrenormalized self energy of the weak gauge boson Z can be written as

$$\Sigma_{\mu\nu}^Z(p) = \Lambda^2 A_0^z g_{\mu\nu} + \left(A_1^z + \frac{p^2}{\Lambda^2} A_2^z \right) (p^2 g_{\mu\nu} - p_\mu p_\nu) + \left(B_1^z + \frac{p^2}{\Lambda^2} B_2^z \right) p_\mu p_\nu . \quad (25)$$

Correspondingly, the counter terms are given as

$$\Sigma_{\mu\nu}^{ZC}(p) = -(\delta m_z^2 + m_z^2 \delta Z_z) g_{\mu\nu} - \delta Z_z (p^2 g_{\mu\nu} - p_\mu p_\nu) . \quad (26)$$

The renormalized self energy is given by

$$\hat{\Sigma}_{\mu\nu}^Z(p) = \Sigma_{\mu\nu}^Z(p) + \Sigma_{\mu\nu}^{ZC}(p) . \quad (27)$$

For on-shell external gauge boson Z , we have [18]

$$\begin{aligned} \hat{\Sigma}_{\mu\nu}^Z(p) \epsilon^\nu(p) \Big|_{p^2=m_z^2} &= 0 , \\ \lim_{p^2 \rightarrow m_z^2} \frac{1}{p^2 - m_z^2} \hat{\Sigma}_{\mu\nu}^Z(p) \epsilon^\nu(p) &= \epsilon_\mu(p) , \end{aligned} \quad (28)$$

where $\epsilon(p)$ is the polarization vector of Z gauge boson. From Eq. (28), we get the counter terms

$$\begin{aligned} \delta Z_z &= A_1^z + \frac{m_z^2}{\Lambda^2} A_2^z = A_1^z + x_z A_2^z , \\ \delta m_z^2 &= A_0^z \Lambda^2 - m_z^2 \delta Z_z . \end{aligned} \quad (29)$$

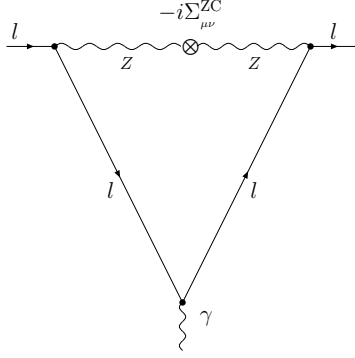


FIG. 2: The counter term diagram to cancel the ultraviolet caused by the self energy of Z boson.

Accordingly, the effective Lagrangian originating from the counter term diagram (Fig.2) can be formulated as

$$\begin{aligned}
\delta\mathcal{L}_{ZZ}^C = & -\frac{e^4}{12(4\pi)^2 s_w^4 c_w^4 \Lambda^2} (4\pi x_R)^{2\varepsilon} \frac{\Gamma^2(1+\varepsilon)}{(1-\varepsilon)^2} \left\{ (\xi_{\beta\alpha}^L \xi_{\alpha\beta}^L + \xi_{\beta\alpha}^R \xi_{\alpha\beta}^R) \left[-\frac{1}{\varepsilon} \frac{x_{x_\alpha^\pm} + x_{x_\beta^\pm}}{x_z^2} \right. \right. \\
& + \frac{5(x_{x_\alpha^\pm} + x_{x_\beta^\pm})}{12x_z^2} + \frac{\varrho_{2,1}(x_{x_\alpha^\pm}, x_{x_\beta^\pm})}{x_z^2} + \frac{5}{12x_z} + \frac{x_{x_\alpha^\pm} + x_{x_\beta^\pm}}{x_z^2} \ln x_R \left. \right] \\
& + 2(x_{x_\alpha^\pm} x_{x_\beta^\pm})^{1/2} (\xi_{\beta\alpha}^L \xi_{\alpha\beta}^R + \xi_{\beta\alpha}^R \xi_{\alpha\beta}^L) \left[\frac{1}{\varepsilon x_z^2} - \frac{\varrho_{1,1}(x_{x_\alpha^\pm}, x_{x_\beta^\pm})}{x_z^2} + \frac{1}{12x_z^2} - \frac{\ln x_R}{x_z^2} \right] \left. \right\} \\
& \times \left[(T_f^Z - Q_f s_w^2)^2 (\mathcal{O}_2^- + \mathcal{O}_3^-) + Q_f^2 s_w^4 (\mathcal{O}_2^+ + \mathcal{O}_3^+) \right] \\
& + \frac{e^4}{4(4\pi)^2 s_w^4 c_w^4 \Lambda^2} (4\pi x_R)^{2\varepsilon} \frac{\Gamma^2(1+\varepsilon)}{(1-\varepsilon)^2} \left\{ (\xi_{\beta\alpha}^L \xi_{\alpha\beta}^L + \xi_{\beta\alpha}^R \xi_{\alpha\beta}^R) \left[\frac{1}{\varepsilon} \frac{x_{x_\alpha^\pm} + x_{x_\beta^\pm}}{x_z^2} \right. \right. \\
& - \frac{\varrho_{2,1}(x_{x_\alpha^\pm}, x_{x_\beta^\pm})}{x_z^2} - \frac{x_{x_\alpha^\pm} + x_{x_\beta^\pm}}{x_z^2} \left(\frac{7}{2} + \ln x_l - \ln x_z \right) + \frac{1}{4x_z} - \frac{x_{x_\alpha^\pm} + x_{x_\beta^\pm}}{x_z^2} \ln x_R \left. \right] \\
& + 2(x_{x_\alpha^\pm} x_{x_\beta^\pm})^{1/2} (\xi_{\beta\alpha}^L \xi_{\alpha\beta}^R + \xi_{\beta\alpha}^R \xi_{\alpha\beta}^L) \left[-\frac{1}{\varepsilon x_z^2} + \frac{\varrho_{1,1}(x_{x_\alpha^\pm}, x_{x_\beta^\pm})}{x_z^2} \right. \\
& \left. \left. + \frac{1}{x_z^2} (3 + \ln x_l - \ln x_z) + \frac{\ln x_R}{x_z^2} \right] \right\} Q_f s_w^2 (T_f^Z - Q_l s_w^2) (\mathcal{O}_6^- + \mathcal{O}_6^+) + \dots \quad (30)
\end{aligned}$$

Here, $\varepsilon = 2 - D/2$ with D representing the time-space dimension, and $x_R = \Lambda_{\text{RE}}^2/\Lambda^2$ (Λ_{RE} denotes the renormalization scale).

As a result of the preparation mentioned above, we can add the contributions from the counter term diagram to cancel the corresponding ultraviolet divergence in bare effective Lagrangian. The resulted theoretical predictions on the lepton MDMs and EDMs are re-

spectively written as

$$\begin{aligned}
a_{l,\chi^\pm}^{ZZ} &= -\frac{e^4 m_l^2}{(4\pi)^4 s_w^4 c_w^4 \Lambda^2} \left\{ (|\xi_{\alpha\beta}^L|^2 + |\xi_{\alpha\beta}^R|^2) [(T_f^Z - Q_f s_w^2)^2 + Q_f^2 s_w^4] \right. \\
&\quad \times \left[\frac{Q_f}{3} (T_5(x_z, x_{\chi_\alpha^\pm}, x_{\chi_\beta^\pm}) + \frac{x_{\chi_\alpha^\pm} + x_{\chi_\beta^\pm}}{x_z^2} \ln x_R) + \frac{1}{4} T_4(x_z, x_{\chi_\alpha^\pm}, x_{\chi_\beta^\pm}) \right] \\
&\quad + \frac{1}{8} (|\xi_{\alpha\beta}^L|^2 - |\xi_{\alpha\beta}^R|^2) [(T_f^Z - Q_f s_w^2)^2 - Q_f^2 s_w^4] T_6(x_z, x_{\chi_\alpha^\pm}, x_{\chi_\beta^\pm}) \\
&\quad - \Re(\xi_{\alpha\beta}^L \xi_{\beta\alpha}^R) [(T_f^Z - Q_f s_w^2)^2 + Q_f^2 s_w^4] (x_{\chi_\alpha^\pm} x_{\chi_\beta^\pm})^{1/2} \\
&\quad \times \left[\frac{1}{4} T_7(x_z, x_{\chi_\alpha^\pm}, x_{\chi_\beta^\pm}) + \frac{4Q_f}{3x_z^2} \ln \frac{x_z}{x_R} - \frac{7Q_f}{3x_z^2} \right] \\
&\quad - (|\xi_{\alpha\beta}^L|^2 + |\xi_{\alpha\beta}^R|^2) s_w^2 (T_f^Z - Q_f s_w^2) \left[\frac{Q_f}{4} T_9(x_z, x_{\chi_\alpha^\pm}, x_{\chi_\beta^\pm}) \right. \\
&\quad - \frac{Q_f^2}{4x_z} + \frac{Q_f^2}{x_z^2} (2 - \ln \frac{x_z}{x_R}) (x_{\chi_\alpha^\pm} + x_{\chi_\beta^\pm}) - \frac{Q_f^2}{2x_z^2} (x_{\chi_\alpha^\pm} \ln x_{\chi_\alpha^\pm} + x_{\chi_\beta^\pm} \ln x_{\chi_\beta^\pm}) \\
&\quad \left. \left. + \frac{Q_f^2}{2x_z^2} \cdot (\varrho_{2,1}(x_{\chi_\alpha^\pm}, x_{\chi_\beta^\pm}) - x_{\chi_\alpha^\pm} x_{\chi_\beta^\pm} \varrho_{0,1}(x_{\chi_\alpha^\pm}, x_{\chi_\beta^\pm})) \right] \right\}, \\
&\quad - 4Q_f^2 \Re(\xi_{\alpha\beta}^L \xi_{\beta\alpha}^R) s_w^2 (T_f^Z - Q_f s_w^2) (x_{\chi_\alpha^\pm} x_{\chi_\beta^\pm})^{1/2} \frac{2 - \ln x_z + \ln x_R}{x_z^2} \Bigg\}, \\
d_{l,\chi^\pm}^{ZZ} &= \frac{e^5 m_l}{(4\pi)^4 s_w^4 c_w^4 \Lambda^2} \cdot \Im(\xi_{\alpha\beta}^L \xi_{\beta\alpha}^R) (x_{\chi_\alpha^\pm} x_{\chi_\beta^\pm})^{1/2} \left\{ Q_f s_w^2 (T_f^Z - Q_f s_w^2) \right. \\
&\quad \times \left(\frac{\partial^2}{\partial x_z \partial x_{\chi_\beta^\pm}} - \frac{\partial^2}{\partial x_z \partial x_{\chi_\alpha^\pm}} \right) \left(\frac{\Phi(x_z, x_{\chi_\alpha^\pm}, x_{\chi_\beta^\pm}) - \varphi_0(x_{\chi_\alpha^\pm}, x_{\chi_\beta^\pm})}{x_z} \right) \\
&\quad \left. - \frac{1}{16} [(T_f^Z - Q_f s_w^2)^2 + Q_f^2 s_w^4] T_8(x_z, x_{\chi_\alpha^\pm}, x_{\chi_\beta^\pm}) \right\}. \tag{31}
\end{aligned}$$

Because a real photon can not be attached to the internal closed neutralino loop, the corresponding effective Lagrangian only contains the corrections to the lepton MDMs:

$$\begin{aligned}
a_{l,\chi^0}^{ZZ} &= -\frac{e^4 Q_f m_l^2}{(4\pi)^4 s_w^4 c_w^4 \Lambda^2} \left\{ -\frac{1}{3} (|\eta_{\alpha\beta}^L|^2 + |\eta_{\alpha\beta}^R|^2) [(T_f^Z - Q_f s_w^2)^2 + Q_f^2 s_w^4] \right. \\
&\quad \times \left(T_5(x_z, x_{\chi_\alpha^0}, x_{\chi_\beta^0}) + \frac{x_{\chi_\alpha^0} + x_{\chi_\beta^0}}{x_z^2} \ln x_R \right) \\
&\quad + \frac{1}{3} \Re(\eta_{\alpha\beta}^L \eta_{\beta\alpha}^R) [(T_f^Z - Q_f s_w^2)^2 + Q_f^2 s_w^4] (x_{\chi_\alpha^0} x_{\chi_\beta^0})^{1/2} \left[\frac{4}{x_z^2} \ln \frac{x_z}{x_R} - \frac{7}{x_z^2} \right] \\
&\quad \left. + \frac{1}{2x_z^2} (|\eta_{\alpha\beta}^L|^2 + |\eta_{\alpha\beta}^R|^2) Q_f s_w^2 (T_f^Z - Q_f s_w^2) \left[\frac{x_z}{2} + (x_{\chi_\alpha^0} \ln x_{\chi_\alpha^0} + x_{\chi_\beta^0} \ln x_{\chi_\beta^0}) \right] \right\}
\end{aligned}$$

$$\begin{aligned}
& \left. -2(x_{x_\alpha^0} + x_{x_\beta^0})(2 - \ln \frac{x_z}{x_R}) - \varrho_{2,1}(x_{x_\alpha^0}, x_{x_\beta^0}) + x_{x_\alpha^0} x_{x_\beta^0} \varrho_{0,1}(x_{x_\alpha^0}, x_{x_\beta^0}) \right] \\
& -4Q_f \Re(\eta_{\alpha\beta}^L \eta_{\beta\alpha}^R) s_w^2 (T_f^Z - Q_f s_w^2) (x_{x_\alpha^0} x_{x_\beta^0})^{1/2} \frac{2 - \ln x_z + \ln x_R}{x_z^2} \Big\} \quad (32)
\end{aligned}$$

with

$$\begin{aligned}
\eta_{\alpha\beta}^L &= \mathcal{N}_{\alpha 4}^\dagger \mathcal{N}_{4\beta}, \\
\eta_{\alpha\beta}^R &= \mathcal{N}_{\beta 3}^\dagger \mathcal{N}_{3\alpha}, \quad (\alpha, \beta = 1, \dots, 4). \quad (33)
\end{aligned}$$

We can also simplify Eq.(31) and Eq.(32) using the asymptotic expressions of $T_8 \sim T_{13}$ in the limit $x_{x_\alpha^\pm}, x_{x_\beta^\pm}, x_{x_\alpha^0}, x_{x_\beta^0} \gg x_z$. The concrete expressions of $T_8 \sim T_{13}$ can be found in appendix.

F. The effective Lagrangian from the WW sector

Similarly, the self energy of W gauge boson composed of a closed chargino-neutralino loop induces the ultraviolet divergence in the Wilson coefficients of effective Lagrangian. Accordingly, the unrenormalized W self energy is expressed as

$$\Sigma_{\mu\nu}^W(p) = \Lambda^2 A_0^w g_{\mu\nu} + \left(A_1^w + \frac{p^2}{\Lambda^2} A_2^w \right) (p^2 g_{\mu\nu} - p_\mu p_\nu) + \left(B_1^w + \frac{p^2}{\Lambda^2} B_2^w \right) p_\mu p_\nu. \quad (34)$$

The corresponding counter terms are given as

$$\Sigma_{\mu\nu}^{\text{WC}}(p) = -(\delta m_w^2 + m_w^2 \delta Z_w) g_{\mu\nu} - \delta Z_w (p^2 g_{\mu\nu} - p_\mu p_\nu). \quad (35)$$

The renormalized self energy is given by

$$\hat{\Sigma}_{\mu\nu}^W(p) = \Sigma_{\mu\nu}^W(p) + \Sigma_{\mu\nu}^{\text{WC}}(p) \quad (36)$$

For on-shell external gauge boson W^\pm , we have [18]

$$\begin{aligned}
& \hat{\Sigma}_{\mu\nu}^W(p) \epsilon^\nu(p) \Big|_{p^2=m_w^2} = 0, \\
& \lim_{p^2 \rightarrow m_w^2} \frac{1}{p^2 - m_w^2} \hat{\Sigma}_{\mu\nu}^W(p) \epsilon^\nu(p) = \epsilon_\mu(p), \quad (37)
\end{aligned}$$

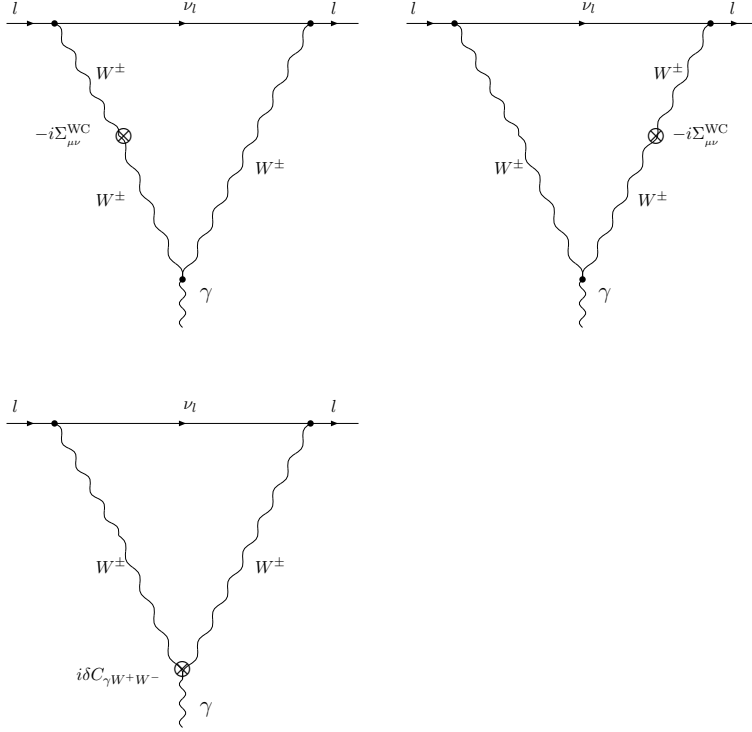


FIG. 3: The counter term diagram to cancel the ultraviolet caused by the self energy of W boson and electroweak radiative corrections to $\gamma W^+ W^-$ vertex.

where $\epsilon(p)$ is the polarization vector of W gauge boson. Inserting Eq. (34) and Eq. (35) into Eq. (37), we derive the counter terms for the W self energy as

$$\begin{aligned} \delta Z_w &= A_1^w + \frac{m_w^2}{\Lambda^2} A_2^w = A_1^w + x_z A_2^w, \\ \delta m_w^2 &= A_0^w \Lambda^2 - m_w^2 \delta Z_w. \end{aligned} \quad (38)$$

Differing from the analysis in the ZZ sector, we should derive the counter term for the vertex $\gamma W^+ W^-$ here since the corresponding coupling is not zero at tree level. In the nonlinear R_ξ gauge with $\xi = 1$, the counter term for the vertex $\gamma W^+ W^-$ is

$$i\delta C_{\gamma W^+ W^-} = ie \cdot \delta Z_w \left[g_{\mu\nu}(k_1 - k_2)_\rho + g_{\nu\rho}(k_2 - k_3)_\mu + g_{\rho\mu}(k_3 - k_1)_\nu \right], \quad (39)$$

where k_i ($i = 1, 2, 3$) denote the injection momenta of W^\pm and photon, and μ, ν, ρ denote the corresponding Lorentz indices respectively.

We present the counter term diagrams to cancel the ultraviolet divergence contained in the bare effective Lagrangian from WW sector in Fig.3, and we can verify that the sum of corresponding amplitude satisfies the Ward identity required by the QED gauge invariance obviously. Accordingly, the effective Lagrangian originating from the counter term diagrams can be written as

$$\begin{aligned}
\delta\mathcal{L}_{ww}^C &= \frac{e^4}{(4\pi)^2 s_w^4 \Lambda^2 Q_f} (4\pi x_R)^{2\varepsilon} \frac{\Gamma^2(1+\varepsilon)}{(1-\varepsilon)^2} \left\{ (\zeta_{\alpha\beta}^{L*} \zeta_{\alpha\beta}^L + \zeta_{\alpha\beta}^{R*} \zeta_{\alpha\beta}^R) \right. \\
&\times \left[\frac{5}{24x_w^2} \left(-\frac{x_{\chi_\alpha^0} + x_{\chi_\beta^\pm}}{\varepsilon} - \frac{x_{\chi_\alpha^0} + x_{\chi_\beta^\pm}}{3} + \varrho_{2,1}(x_{\chi_\alpha^0}, x_{\chi_\beta^\pm}) \right) \right. \\
&+ (x_{\chi_\alpha^0} + x_{\chi_\beta^\pm}) \ln x_R \left. \right] + \frac{11}{36x_w} \left. \right] (\mathcal{O}_2^- + \mathcal{O}_3^-) \\
&+ (\zeta_{\alpha\beta}^{L*} \zeta_{\alpha\beta}^R + \zeta_{\alpha\beta}^{R*} \zeta_{\alpha\beta}^L) (x_{\chi_\alpha^0} x_{\chi_\beta^\pm})^{1/2} \left[\frac{5}{12x_w^2} \left(\frac{1}{\varepsilon} + \frac{5}{6} - \varrho_{1,1}(x_{\chi_\alpha^0}, x_{\chi_\beta^\pm}) \right) \right. \\
&\left. \left. - \ln x_R \right] (\mathcal{O}_2^- + \mathcal{O}_3^-) \right\} + \dots . \tag{40}
\end{aligned}$$

Finally, we get the renormalized effective Lagrangian from the WW sector:

$$\begin{aligned}
\mathcal{L}_{ww} &= -\frac{e^4}{48(4\pi)^2 s_w^4 Q_f \Lambda^2} (\zeta_{\alpha\beta}^{L*} \zeta_{\alpha\beta}^L + \zeta_{\alpha\beta}^{R*} \zeta_{\alpha\beta}^R) \left[T_{10}(x_w, x_{\chi_\alpha^0}, x_{\chi_\beta^\pm}) \right. \\
&+ \frac{10}{x_w^2} (x_{\chi_\alpha^0} + x_{\chi_\beta^\pm}) \ln x_R \left. \right] (\mathcal{O}_2^- + \mathcal{O}_3^-) \\
&- \frac{e^4}{16(4\pi)^2 s_w^4 Q_f \Lambda^2} (\zeta_{\alpha\beta}^{L*} \zeta_{\alpha\beta}^L - \zeta_{\alpha\beta}^{R*} \zeta_{\alpha\beta}^R) T_{11}(x_w, x_{\chi_\alpha^0}, x_{\chi_\beta^\pm}) (\mathcal{O}_2^- + \mathcal{O}_3^-) \\
&- \frac{e^4 (x_{\chi_\alpha^0} x_{\chi_\beta^\pm})^{1/2}}{48(4\pi)^2 s_w^4 Q_f \Lambda^2} (\zeta_{\alpha\beta}^{L*} \zeta_{\alpha\beta}^R + \zeta_{\alpha\beta}^{R*} \zeta_{\alpha\beta}^L) \left[T_{12}(x_w, x_{\chi_\alpha^0}, x_{\chi_\beta^\pm}) - \frac{20}{x_w^2} \ln x_R \right] (\mathcal{O}_2^- + \mathcal{O}_3^-) \\
&- \frac{e^4 (x_{\chi_\alpha^0} x_{\chi_\beta^\pm})^{1/2}}{16(4\pi)^2 s_w^4 Q_f \Lambda^2} (\zeta_{\alpha\beta}^{R*} \zeta_{\alpha\beta}^L - \zeta_{\alpha\beta}^{L*} \zeta_{\alpha\beta}^R) T_{13}(x_w, x_{\chi_\alpha^0}, x_{\chi_\beta^\pm}) (\mathcal{O}_2^- - \mathcal{O}_3^-) . \tag{41}
\end{aligned}$$

Correspondingly, the resulted lepton MDMs and EDMs are respectively formulated as

$$\begin{aligned}
a_l^{WW} &= -\frac{e^4 m_l^2}{12(4\pi)^4 s_w^4 \Lambda^2} (|\zeta_{\alpha\beta}^L|^2 + |\zeta_{\alpha\beta}^R|^2) \left[T_{10}(x_w, x_{\chi_\alpha^0}, x_{\chi_\beta^\pm}) \right. \\
&+ \frac{10}{x_w^2} (x_{\chi_\alpha^0} + x_{\chi_\beta^\pm}) \ln x_R - \frac{32}{x_w} \ln x_R \left. \right] \\
&- \frac{e^4 m_l^2}{4(4\pi)^4 s_w^4 \Lambda^2} (|\zeta_{\alpha\beta}^L|^2 - |\zeta_{\alpha\beta}^R|^2) T_{11}(x_w, x_{\chi_\alpha^0}, x_{\chi_\beta^\pm})
\end{aligned}$$

$$\begin{aligned}
& -\frac{e^4 m_l^2 (x_{x_\alpha^0} x_{x_\beta^\pm})^{1/2}}{6(4\pi)^4 s_w^4 \Lambda^2} \Re(\zeta_{\alpha\beta}^{R*} \zeta_{\alpha\beta}^L) \left[T_{12}(x_w, x_{x_\alpha^0}, x_{x_\beta^\pm}) - \frac{20}{x_w^2} \ln x_R \right], \\
d_l^{WW} = & -\frac{e^5 m_l (x_{x_\alpha^0} x_{x_\beta^\pm})^{1/2}}{4(4\pi)^4 s_w^4 \Lambda^2} \Im(\zeta_{\alpha\beta}^{R*} \zeta_{\alpha\beta}^L) T_{13}(x_w, x_{x_\alpha^0}, x_{x_\beta^\pm}). \tag{42}
\end{aligned}$$

III. NUMERICAL RESULTS AND DISCUSSION

With the theoretical formulae derived in previous section, we numerically analyze the dependence of the muon MDM and the electron EDM on the supersymmetric parameters in the split scenario here. In particular, we will present the dependence of the muon MDM and the electron EDM on the supersymmetric CP phases in some detail. Within three standard error deviations, the present experimental data can tolerate new physics corrections to the muon MDM as $-10 \times 10^{-10} < \Delta a_\mu < 52 \times 10^{-10}$. Since the neutralinos χ_α^0 ($\alpha = 1, 2, 3, 4$) and charginos χ_α^\pm ($\alpha = 1, 2$) appear as the internal intermediate particles in the two-loop diagrams which are investigated in this work, the corrections of these diagrams will be suppressed strongly when the masses of neutralinos and charginos are much higher than the electroweak scale[11]. To investigate if those diagrams can result in concrete corrections to the muon MDM and electron EDM, we choose a suitable supersymmetric parameter region where the masses of neutralinos and charginos are lying in the range $M_\chi < 500$ GeV. Without losing too much generality, we assume the supersymmetric parameters satisfying $|m_1| = |m_2|$ in this work. In split SUSY, only the CP violating phases $\arg(\mu_H)$, $\arg(m_1)$, and $\arg(m_2)$ have substantive contributions to the lepton MDMs and EDMs. As for other CP violating phases, either they do not contribute to the lepton MDMs and EDMs or their corrections can be neglected safely. Moreover, the existence of a CP-even SM like Higgs with mass around 100 – 250 GeV sets a strong constraint on the parameter space of the employed model. To address this problem, they argue that a fine tuning in the Higgs potential is required [25]. Admitting this fine tuning among high energy scale parameters, one no longer worries about the constraint from Higgs sector. On the other hand, the CP violation would cause changes to the neutral-Higgs-quark coupling, the neutral Higgs-gauge-boson coupling and the self-coupling of Higgs boson. The present experimental lower bound on the mass

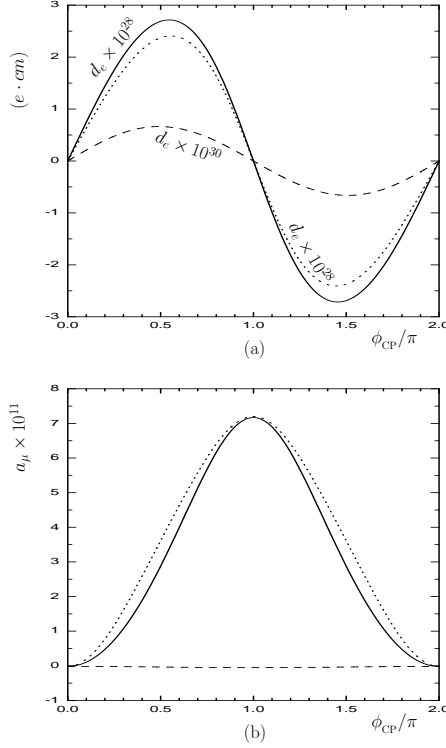


FIG. 4: The supersymmetric corrections to the electron EDM d_e and muon MDM a_μ vary with the CP violating phase ϕ_{CP} when $|\mu_H| = |m_1| = |m_2| = 200$ GeV and $\tan\beta = 5$. Where the dash lines stand for the corrections with $\phi_{\text{CP}} = \arg(m_1)$ and $\arg(m_2) = \arg(\mu_H) = 0$, the dot lines stand for the corrections with $\phi_{\text{CP}} = \arg(m_2)$ and $\arg(m_1) = \arg(\mu_H) = 0$, and the solid lines stand for the corrections with $\phi_{\text{CP}} = \arg(\mu_H)$ and $\arg(m_1) = \arg(m_2) = 0$, respectively.

of the lightest Higgs bosons is relaxed to 60 GeV [26]. The scope of Higgs mass is chosen around 60 – 250 GeV in our numerical analysis because of the above reasons. In fact, we find that the lepton MDMs and EDMs weakly depend on the mass of lightest Higgs by scanning the parameter space. In the following discussion, we choose the mass of light Higgs as $m_h = 120$ GeV.

Taking $|\mu_H| = |m_1| = |m_2| = 200$ GeV and $\tan\beta = 5$, we plot the electron EDM d_e and muon MDM a_μ versus the CP phases $\phi_{\text{CP}} = \arg(m_1)$, $\arg(m_2)$, $\arg(\mu_H)$ separately in Fig.4. When $\arg(m_2) = \arg(\mu_H) = 0$, there is cancellation among the dominant contributions to a_μ that originate from the " γZ " and " ZZ " sectors respectively. As $\phi_{\text{CP}} = \arg(\mu_H)$ and $\arg(m_1) = \arg(m_2) = 0$, the absolute values of supersymmetric corrections to the electron EDM d_e (solid line in Fig.4(a)) exceed $2.5 \times 10^{-28} e \cdot \text{cm}$ at the largest CP violation $\arg(\mu_H) = \pi/2, 3\pi/2$, which is well below the present experimental upper limit $1.7 \times 10^{-27} e \cdot \text{cm}$ [21],

but large enough to be detected in next generation experiments. Correspondingly, the muon MDM a_μ depends on the CP violating phase $\phi_{\text{CP}} = \arg(\mu_H)$ (solid line in Fig.4(b)) strongly, the supersymmetric corrections to a_μ exceed 3×10^{-11} at the largest CP violation ($\arg(\mu_H) = \pi/2, 3\pi/2$) since the cancellation mentioned above dissolves now. For the same reason, the supersymmetric correction to a_μ surpasses 7×10^{-11} at the CP conservation of $\arg(\mu_H) = \pi$. As $\phi_{\text{CP}} = \arg(m_2)$ and $\arg(m_1) = \arg(\mu_H) = 0$, the absolute values of supersymmetric corrections to the electron EDM d_e (solid line in Fig.4(a)) exceed $2 \times 10^{-28} e \cdot cm$ at the largest CP violation $\arg(\mu_H) = \pi/2, 3\pi/2$, which is expected to be observed in next generation experiments with the sensitivity $10^{-29} e \cdot cm$ [22]. Correspondingly, the muon MDM a_μ depends on the CP violating phase $\phi_{\text{CP}} = \arg(m_2)$ (dot line in Fig.4(b)) sensitively, the supersymmetric corrections to a_μ are about 3×10^{-11} at the largest CP violation ($\arg(\mu_H) = \pi/2, 3\pi/2$) because the cancellation existing as $\arg(m_2) = \arg(\mu_H) = 0$ vanishes here. When $\phi_{\text{CP}} = \arg(m_1)$ and $\arg(m_2) = \arg(\mu_H) = 0$, the supersymmetric correction to the electron EDM d_e (dash line in Fig.4(a)) is below $1 \times 10^{-30} e \cdot cm$, and very difficult to be detected in near future. Corresponding to small theoretical prediction on the electron EDM d_e , the muon MDM a_μ varies with the CP phase $\phi_{\text{CP}} = \arg(m_1)$ (dash line Fig.4(b)) very mildly.

Taking $|\mu_H| = |m_1| = |m_2| = 200 \text{ GeV}$ and $\tan \beta = 50$, we plot the electron EDM d_e and muon MDM a_μ versus the CP phases $\phi_{\text{CP}} = \arg(m_1), \arg(m_2), \arg(\mu_H)$ separately in Fig.5. As $\phi_{\text{CP}} = \arg(\mu_H)$ and $\arg(m_1) = \arg(m_2) = 0$, the absolute values of supersymmetric corrections to the electron EDM d_e (solid line in Fig.5(a)) reach $3 \times 10^{-28} e \cdot cm$ at the largest CP violation $\arg(\mu_H) = \pi/2, 3\pi/2$, which exceeds the precision of next generation experiments[22]. Correspondingly, the muon MDM a_μ depends on the CP violating phase $\phi_{\text{CP}} = \arg(\mu_H)$ (solid line in Fig.5(b)) strongly, the supersymmetric corrections to a_μ are about 3×10^{-11} at the largest CP violation ($\arg(\mu_H) = \pi/2, 3\pi/2$) since the cancellation appearing at $\arg(m_2) = \arg(\mu_H) = 0$ dissolves here. As $\phi_{\text{CP}} = \arg(m_2)$ and $\arg(m_1) = \arg(\mu_H) = 0$, the absolute values of supersymmetric corrections to the electron EDM d_e (solid line in Fig.5(a)) exceed $2.5 \times 10^{-28} e \cdot cm$ at the largest CP violation $\arg(\mu_H) = \pi/2, 3\pi/2$, which is expected to be observed in next generation experiments with the sensitivity $10^{-29} e \cdot cm$. Correspondingly, the muon MDM a_μ depends on the CP violating phase $\phi_{\text{CP}} = \arg(m_2)$ (dot line in Fig.5(b)) steeply, the supersymmetric corrections to a_μ are about 4×10^{-11} at the

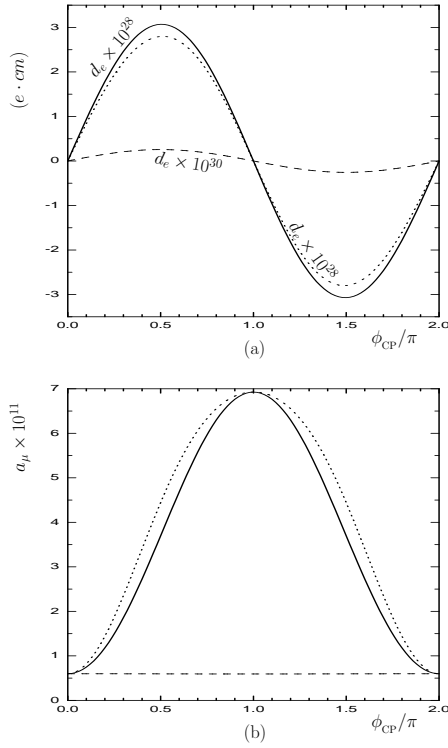


FIG. 5: The supersymmetric corrections to the electron EDM d_e and muon MDM a_μ vary with the CP violating phase ϕ_{CP} when $|\mu_H| = |m_1| = |m_2| = 200$ GeV and $\tan\beta = 50$. Where the dash lines stand for the corrections with $\phi_{\text{CP}} = \arg(m_1)$ and $\arg(m_2) = \arg(\mu_H) = 0$, the dot lines stand for the corrections with $\phi_{\text{CP}} = \arg(m_2)$ and $\arg(m_1) = \arg(\mu_H) = 0$, and the solid lines stand for the corrections with $\phi_{\text{CP}} = \arg(\mu_H)$ and $\arg(m_1) = \arg(m_2) = 0$, separately.

largest CP violation ($\arg(\mu_H) = \pi/2, 3\pi/2$) because the cancellation existing at $\arg(m_2) = \arg(\mu_H) = 0$ disappears presently. When $\phi_{\text{CP}} = \arg(m_1)$ and $\arg(m_2) = \arg(\mu_H) = 0$, the supersymmetric correction to the electron EDM d_e (dash line in Fig.5(a)) is less than $1 \times 10^{-30} e \cdot \text{cm}$, and very difficult to be detected in near future. Corresponding to small theoretical prediction on the electron EDM d_e , the muon MDM a_μ varies with the CP phase $\phi_{\text{CP}} = \arg(m_1)$ (dash line Fig.5(b)) very slowly.

Note that the theoretical predictions on the electron EDM d_e and muon MDM a_μ are not enhanced by large $\tan\beta$ here, this point can be understood as follows. The $\tan\beta$ enhanced couplings are only contained in the interactions among the heavy Higgs and down-type fermions (sfermions). Those heavy Higgs fields include the neutral CP-odd Higgs, the neutral heavy CP-even Higgs, as well as the charged Higgs. However, those particles are decoupled from the low energy theory because they are super-heavy under the split assumption. In

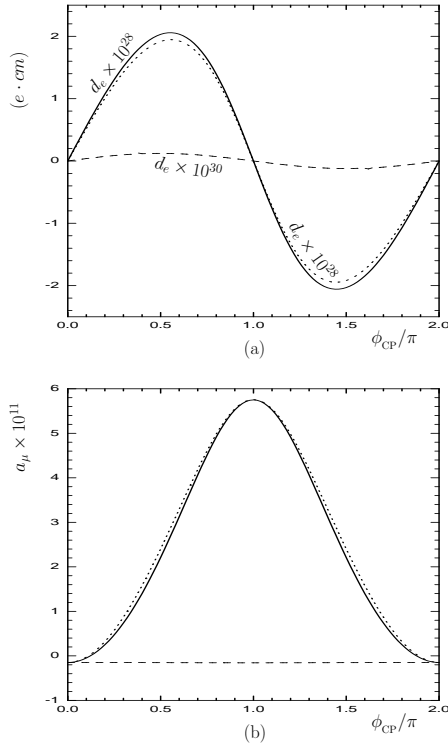


FIG. 6: The supersymmetric corrections to the electron EDM d_e and muon MDM a_μ vary with the CP violating phase ϕ_{CP} when $|\mu_H| = |m_1| = |m_2| = 300$ GeV and $\tan\beta = 5$. Where the dash lines stand for the corrections with $\phi_{\text{CP}} = \arg(m_1)$ and $\arg(m_2) = \arg(\mu_H) = 0$, the dot lines stand for the corrections with $\phi_{\text{CP}} = \arg(m_2)$ and $\arg(m_1) = \arg(\mu_H) = 0$, and the solid lines stand for the corrections with $\phi_{\text{CP}} = \arg(\mu_H)$ and $\arg(m_1) = \arg(m_2) = 0$, separately.

other words, our theoretical predictions are not enhanced by large $\tan\beta$ since we ignore the corrections from those heavy Higgs fields.

Taking $|\mu_H| = |m_1| = |m_2| = 300$ GeV and $\tan\beta = 5$, we plot the electron EDM d_e and muon MDM a_μ versus the CP phases $\phi_{\text{CP}} = \arg(m_1)$, $\arg(m_2)$, $\arg(\mu_H)$ separately in Fig.6. As $\arg(m_2) = \arg(\mu_H) = 0$, a cancellation exists among the dominant supersymmetric contributions to a_μ that originate from the " γZ " and " ZZ " sectors respectively. When $\phi_{\text{CP}} = \arg(\mu_H)$ and $\arg(m_1) = \arg(m_2) = 0$, the absolute values of supersymmetric corrections to the electron EDM d_e (solid line in Fig.6(a)) approach $2 \times 10^{-28} e \cdot \text{cm}$ at the largest CP violation $\arg(\mu_H) = \pi/2, 3\pi/2$, which is well below the present experimental upper limit $1.7 \times 10^{-27} e \cdot \text{cm}$, but large enough to be detected in next generation experiments with the precision of $10 \times 10^{-29} e \cdot \text{cm}$. Correspondingly, the muon MDM a_μ depends on the CP violating phase $\phi_{\text{CP}} = \arg(\mu_H)$ (solid line in Fig.6(b)) strongly, the supersymmetric

corrections to a_μ exceed 2×10^{-11} at the largest CP violation ($\arg(\mu_H) = \pi/2, 3\pi/2$) since the cancellation mentioned above dissolves here. For the same reason, the supersymmetric correction to a_μ surpasses 5.5×10^{-11} at the CP conservation of $\arg(\mu_H) = \pi$. As $\phi_{\text{CP}} = \arg(m_2)$ and $\arg(m_1) = \arg(\mu_H) = 0$, the absolute values of supersymmetric corrections to the electron EDM d_e (solid line in Fig.6(a)) exceed $2 \times 10^{-28} e \cdot \text{cm}$ at the largest CP violation $\arg(\mu_H) = \pi/2, 3\pi/2$, which is expected to be observed in next generation experiments. Correspondingly, the muon MDM a_μ depends on the CP violating phase $\phi_{\text{CP}} = \arg(m_2)$ (dot line in Fig.6(b)) steeply, the supersymmetric corrections to a_μ are about 2×10^{-11} at the largest CP violation ($\arg(\mu_H) = \pi/2, 3\pi/2$) because the cancellation appearing at $\arg(m_2) = \arg(\mu_H) = 0$ vanishes now. When $\phi_{\text{CP}} = \arg(m_1)$ and $\arg(m_2) = \arg(\mu_H) = 0$, the supersymmetric correction to the electron EDM d_e (dash line in Fig.6(a)) is below $1 \times 10^{-30} e \cdot \text{cm}$, and very difficult to be detected in near future. Corresponding to small theoretical prediction on the electron EDM d_e , the muon MDM a_μ varies with the CP phase $\phi_{\text{CP}} = \arg(m_1)$ (dash line Fig.6(b)) very slowly.

Taking $|\mu_H| = |m_1| = |m_2| = 300 \text{ GeV}$ and $\tan \beta = 50$, we plot the electron EDM d_e and muon MDM a_μ versus the CP phases $\phi_{\text{CP}} = \arg(m_1), \arg(m_2), \arg(\mu_H)$ separately in Fig.7. As $\phi_{\text{CP}} = \arg(\mu_H)$ and $\arg(m_1) = \arg(m_2) = 0$, the absolute values of supersymmetric corrections to the electron EDM d_e (solid line in Fig.5(a)) reach $2.3 \times 10^{-28} e \cdot \text{cm}$ at the largest CP violation $\arg(\mu_H) = \pi/2, 3\pi/2$, which exceeds the precision of next generation experiments. Correspondingly, the muon MDM a_μ depends on the CP violating phase $\phi_{\text{CP}} = \arg(\mu_H)$ (solid line in Fig.7(b)) strongly, the supersymmetric corrections to a_μ are about 2×10^{-11} at the largest CP violation ($\arg(\mu_H) = \pi/2, 3\pi/2$) since the cancellation existing at $\arg(m_2) = \arg(\mu_H) = 0$ dissolves here. As $\phi_{\text{CP}} = \arg(m_2)$ and $\arg(m_1) = \arg(\mu_H) = 0$, the absolute values of supersymmetric corrections to the electron EDM d_e (solid line in Fig.7(a)) exceed $2.2 \times 10^{-28} e \cdot \text{cm}$ at the largest CP violation $\arg(\mu_H) = \pi/2, 3\pi/2$, which is expected to be observed in next generation experiments. Correspondingly, the muon MDM a_μ depends on the CP violating phase $\phi_{\text{CP}} = \arg(m_2)$ (dot line in Fig.7(b)) steeply, the supersymmetric corrections to a_μ are about 2×10^{-11} at the largest CP violation ($\arg(\mu_H) = \pi/2, 3\pi/2$) because the cancellation mentioned above vanishes also now. When $\phi_{\text{CP}} = \arg(m_1)$ and $\arg(m_2) = \arg(\mu_H) = 0$, the supersymmetric correction to the electron EDM d_e (dash line

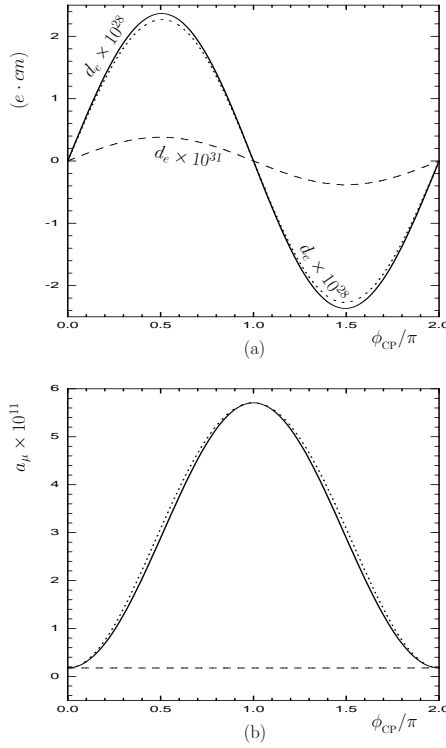


FIG. 7: The supersymmetric corrections to the electron EDM d_e and muon MDM a_μ vary with the CP violating phase ϕ_{CP} when $|\mu_H| = |m_1| = |m_2| = 300$ GeV and $\tan\beta = 50$. Where the dash lines stand for the corrections with $\phi_{\text{CP}} = \arg(m_1)$ and $\arg(m_2) = \arg(\mu_H) = 0$, the dot lines stand for the corrections with $\phi_{\text{CP}} = \arg(m_2)$ and $\arg(m_1) = \arg(\mu_H) = 0$, and the solid lines stand for the corrections with $\phi_{\text{CP}} = \arg(\mu_H)$ and $\arg(m_1) = \arg(m_2) = 0$, respectively.

in Fig.7(a)) is less than $1 \times 10^{-31} e \cdot \text{cm}$, and very difficult to be detected in near future. Corresponding to small theoretical prediction on the electron EDM d_e , the muon MDM a_μ varies with the CP phase $\phi_{\text{CP}} = \arg(m_1)$ (dash line Fig.7(b)) very mildly.

In the numerical analysis presented above, the assumption $|\mu_H| = |m_1| = |m_2|$ is taken for simplicity. This assumption on parameter space induces very specific mixing patterns in chargino and neutralino sectors respectively. In order to investigate the supersymmetric corrections to a_μ and d_e without the assumption, we plot a_μ and d_e varying with the energy scale of new physics Λ_{NP} when $\arg(\mu_H) = \arg(m_1) = 0$, $\arg(m_2) = \pi/2$ in Fig.8. Because the supersymmetric corrections to a_μ and d_e depend on $\tan\beta$ mildly, we choose a middle value of $\tan\beta = 20$. In Fig.8(a) and Fig.8(b), the solid lines stand for the supersymmetric corrections with $|\mu_H| = |m_1| = |m_2| = \Lambda_{\text{NP}}$, the dot lines stand for the supersymmetric corrections with $|\mu_H| = 200$ GeV, $|m_1| = |m_2| = \Lambda_{\text{NP}}$, and the dash lines stand for the supersymmetric

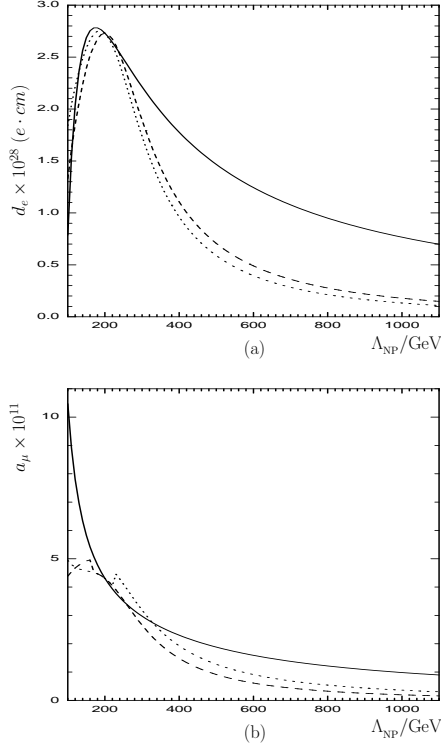


FIG. 8: The supersymmetric corrections to the electron EDM d_e and muon MDM a_μ vary with the energy scale Λ when $\tan \beta = 20$, and $\arg(\mu_H) = \arg(m_1) = 0$, $\arg(m_2) = \pi/2$. Where the dot lines stand for the corrections with $|\mu_H| = 200$ GeV, $|m_1| = |m_2| = \Lambda_{\text{NP}}$, the dash lines stand for the corrections with $|m_1| = |m_2| = 200$ GeV, $|\mu_H| = \Lambda_{\text{NP}}$, and the solid lines stand for the corrections with $|\mu_H| = |m_1| = |m_2| = \Lambda_{\text{NP}}$, respectively.

corrections with $|m_1| = |m_2| = 200$ GeV, $|\mu_H| = \Lambda_{\text{NP}}$, respectively. In Fig.8(a), the resonance around $\Lambda_{\text{NP}} = 200$ GeV is arisen by the intervention between the standard and supersymmetric fields. As $\Lambda_{\text{NP}} \leq 350$ GeV, the difference between the theoretical predictions on d_e with and without $|\mu_H| = |m_1| = |m_2|$ is not very obvious. With the increasing of Λ_{NP} , the suppression of supersymmetric correction to d_e without the assumption is more stronger than that with the assumption. A similar case exists in the 2-loop electroweak correction to a_μ , the suppression of supersymmetric correction to a_μ without the assumption is stronger than that with the assumption when the energy scale Λ_{NP} increases.

IV. CONCLUSIONS

In this work, we analyzed the two-loop supersymmetric corrections to the muon MDM and electron EDM by the effective Lagrangian method in split scenarios. In the concrete calculation, we keep all dimension 6 operators. The ultraviolet divergence caused by the divergent sub-diagrams is removed in the on-shell renormalization schemes. After applying the equations of motion to the external leptons, we derive the muon MDM and the electron EDM. Numerically, we analyze the dependence of the muon MDM a_μ as well as the electron EDM d_e on supersymmetric CP violating phases. Adopting our assumptions on parameter space of the split supersymmetry, we find that the correction from those two-loop diagrams to a_μ is below 10^{-10} roughly for CP conservation, which is less than the present experimental precision in magnitude. In other words, the present experimental data do not put a very restrictive bound on parameter space of split supersymmetry. Additional, the contribution to d_μ from this sector is sizable enough to be experimentally detected with the experimental precision of near future.

Acknowledgments

The work has been supported by the National Natural Science Foundation of China (NNSFC) with No. 10675027. One of us (TFF) also acknowledges the support from the ABRL Grant No. R14-2003-012-01001-0 of Korea at the early stage of this work.

APPENDIX A: THE FUNCTIONS

We list the tedious expressions of the functions adopted in the text

$$\varrho_{i,j}(x,y) = \frac{x^i \ln^j x - y^i \ln^j y}{x-y},$$
$$\Omega_n(x,y;u,v) = \frac{x^n \Phi(x,u,v) - y^n \Phi(y,u,v)}{x-y},$$

$$T_1(x_1, x_2, x_3) = \frac{1}{x_1} \left\{ -4(2 + \ln x_2)(\ln x_1 - 1) - \frac{\partial}{\partial x_3} \left[\left(1 + 2\frac{x_2 - x_3}{x_1}\right) \Phi \right] (x_1, x_2, x_3) \right. \\ \left. + \frac{\partial}{\partial x_3} \left[\left(1 + 2\frac{x_2 - x_3}{x_1}\right) \varphi_0 + 2(x_2 - x_3) \varphi_1 \right] (x_2, x_3) \right\},$$

$$T_2(x_1, x_2, x_3) = \frac{1}{x_1} \left[\frac{\partial \Phi}{\partial x_3} (x_1, x_2, x_3) - \frac{\partial \varphi_0}{\partial x_3} (x_2, x_3) \right],$$

$$T_3(x_1, x_2, x_3) = -\frac{2}{x_1} (2 + \ln x_3) + \frac{2}{x_1} \frac{\partial^2}{\partial x_3^2} (x_3 \Phi) (x_1, x_2, x_3) \\ - \frac{2}{x_1} \frac{\partial^2}{\partial x_3^2} (x_3 \varphi_0) (x_2, x_3) - \frac{4}{x_1} \frac{\partial \Phi}{\partial x_3} (x_1, x_2, x_3) \\ + \frac{4}{x_1} \frac{\partial \varphi_0}{\partial x_3} (x_2, x_3) + \frac{\partial^2}{\partial x_1 \partial x_3} \left(\frac{x_2 - x_3}{x_1} \varphi_0 \right) (x_2, x_3) \\ + \frac{\partial^2}{\partial x_1 \partial x_3} \left[\left(1 - \frac{x_2 - x_3}{x_1}\right) \Phi \right] (x_1, x_2, x_3),$$

$$T_4(x_1, x_2, x_3) = \frac{2}{x_1} \ln x_3 - \frac{2}{x_1^2} (x_2 - x_2 \ln x_2 - x_3 + x_3 \ln x_3) \\ - \frac{\partial^3}{\partial x_1 \partial x_3^2} \left[\frac{x_2 x_3 - x_3^2}{x_1} (\Phi(x_1, x_2, x_3) - \varphi_0(x_2, x_3)) \right] \\ + \frac{1}{2} \frac{\partial^3}{\partial x_1^2 \partial x_3} \left[(x_2 - 3x_3 - x_1) \Phi(x_1, x_2, x_3) \right] \\ - \frac{1}{2} \frac{\partial^2}{\partial x_1 \partial x_3} \left[\Phi(x_1, x_2, x_3) - \frac{5}{x_1} (x_2 - x_3) (\Phi(x_1, x_2, x_3) \right. \\ \left. - \varphi_0(x_2, x_3)) \right] - \frac{\partial^2}{\partial x_1^2} \left[\frac{x_2 - x_3}{x_1} (\Phi(x_1, x_2, x_3) - \varphi_0(x_2, x_3)) \right] \\ + 2\Phi(x_1, x_2, x_3)],$$

$$T_5(x_1, x_2, x_3) = \frac{5}{12x_1} + \left(\frac{5}{12x_1^2} + \frac{\ln x_1}{3x_1^2} \right) (x_2 + x_3) \\ + \left(\frac{7}{6x_1^2} + \frac{2}{3x_1^2} \ln x_1 \right) (x_2 \ln x_2 + x_3 \ln x_3) \\ + \left(\frac{2}{3x_1^3} - \frac{4}{3x_1^3} \ln x_1 \right) (x_2 - x_3)^2 (1 + \varrho_{1,1}(x_2, x_3)) \\ + \frac{23}{6x_1^2} (x_2 + x_3) (1 + \varrho_{1,1}(x_2, x_3)) - \frac{5\varrho_{2,1}(x_2, x_3)}{x_1^2} \\ - \frac{1}{3x_1^2} \left(1 - \frac{2(x_2 + x_3)}{x_1} \right) (\Phi(x_1, x_2, x_3) - \varphi_0(x_2, x_3)) \\ + \frac{1}{3x_1} \left(\frac{x_2 + x_3}{x_1} - \frac{2(x_2 - x_3)^2}{x_1^2} \right) \varphi_1(x_2, x_3)$$

$$\begin{aligned}
& + \frac{1}{3x_1} \left(1 - \frac{3(x_2 + x_3)}{x_1} + \frac{2(x_2 - x_3)^2}{x_1^2} \right) \frac{\partial \Phi}{\partial x_1}(x_1, x_2, x_3) \\
& - \frac{1}{3} \left(1 - \frac{2(x_2 + x_3)}{x_1} + \frac{(x_2 - x_3)^2}{x_1^2} \right) \frac{\partial^2 \Phi}{\partial x_1^2}(x_1, x_2, x_3) \\
& - \frac{(x_2 - x_3)^2}{3x_1^2} \varphi_2(x_2, x_3), \\
T_6(x_1, x_2, x_3) &= -\frac{1}{x_1^2} \left(\varphi_0 - (x_2 - x_3) \frac{\partial \varphi_0}{\partial x_3} \right)(x_2, x_3) + \left[2x_3 \frac{\partial^3 \Phi}{\partial x_1 \partial x_3^2} + \frac{\partial^2 \Phi}{\partial x_1^2} \right. \\
& + (x_1 - x_2 + x_3) \frac{\partial^3 \Phi}{\partial x_1^2 \partial x_3} + \frac{\Phi}{x_1^2} - \frac{x_2 - x_3}{x_1^2} \frac{\partial \Phi}{\partial x_3} - \frac{1}{x_1} \frac{\partial \Phi}{\partial x_1} \\
& \left. + \left(1 + \frac{x_2 - x_3}{x_1} \right) \frac{\partial^2 \Phi}{\partial x_1 \partial x_3} \right](x_1, x_2, x_3), \\
T_7(x_1, x_2, x_3) &= -2 \frac{\partial^3 \Phi}{\partial x_1^2 \partial x_3}(x_1, x_2, x_3) + \frac{2}{x_1 x_3} - \frac{2}{x_1^2} (\ln x_2 - \ln x_3) \\
& + \left(\frac{\partial^3}{\partial x_1^2 \partial x_3} - \frac{\partial^3}{\partial x_1 \partial x_3^2} + \frac{\partial^3}{\partial x_1^2 \partial x_2} + \frac{\partial^3}{\partial x_1 \partial x_2 \partial x_3} \right) \left[\Phi(x_1, x_2, x_3) \right. \\
& \left. - \frac{x_2 - x_3}{x_1} (\Phi(x_1, x_2, x_3) - \varphi_0(x_2, x_3)) \right], \\
T_8(x_1, x_2, x_3) &= -4 \left(\frac{\partial^3 \Phi}{\partial x_1^2 \partial x_3} + \frac{\partial^3 \Phi}{\partial x_1^2 \partial x_2} \right)(x_1, x_2, x_3) + \frac{4}{x_1 x_3} + \frac{2}{x_1^2} (2 + \ln x_2) \\
& + \left(2 \frac{\partial^3}{\partial x_1 \partial x_3^2} + \frac{\partial^3}{\partial x_1^2 \partial x_2} \right) \left[\frac{x_2 - x_3}{x_1} (\Phi(x_1, x_2, x_3) - \varphi_0(x_2, x_3)) \right. \\
& \left. - \Phi(x_1, x_2, x_3) \right], \\
T_9(x_1, x_2, x_3) &= \frac{2}{x_1} \ln x_3 - \frac{4x_3}{x_1^2} \left(\frac{\partial \Phi}{\partial x_3}(x_1, x_2, x_3) - \frac{\partial \varphi_0}{\partial x_3}(x_2, x_3) \right) \\
& + \frac{\partial^2}{\partial x_1 \partial x_3} \left((x_2 - x_3) \frac{\Phi(x_1, x_2, x_3) - \varphi_0(x_2, x_3)}{x_1} - \Phi(x_1, x_2, x_3) \right) \\
& + \frac{4}{x_1} \left(\frac{\partial \Phi}{\partial x_3} - \frac{\partial \Phi}{\partial x_1} \right)(x_1, x_2, x_3) + \frac{4x_3}{x_1} \frac{\partial^2 \Phi}{\partial x_1 \partial x_3}(x_1, x_2, x_3), \\
T_{10}(x_1, x_2, x_3) &= \frac{26}{x_1} + \frac{17x_2}{x_1^2} + \frac{29x_3}{x_1^2} + \frac{10}{x_1^2} \varrho_{2,1}(x_2, x_3) - \frac{16(x_2 - x_3)^2}{x_1^3} \\
& - \frac{10(x_2 + x_3)}{x_1^2} \ln x_1 - \frac{6 \ln x_3}{x_1} + \left[14 - \frac{16(x_2 - x_3)}{x_1} \right] \frac{x_2 \ln x_2}{x_1^2} \\
& + \left[-4 + \frac{16(x_2 - x_3)}{x_1} \right] \frac{x_3 \ln x_3}{x_1^2} + \left[(x_2 - x_3)^2 - x_1^2 \right] \frac{\partial^4 \Phi}{\partial x_1^4}(x_1, x_2, x_3) \\
& + \left[-5x_1 + 6x_2 + \frac{3(x_2 - x_3)^2}{x_1} \right] \frac{\partial^3 \Phi}{\partial x_1^3}(x_1, x_2, x_3) \\
& + \left[-\frac{9(x_2 - x_3)^2}{x_1^2} + \frac{6x_2}{x_1} + \frac{3x_3}{x_1} \right] \frac{\partial^2 \Phi}{\partial x_1^2}(x_1, x_2, x_3)
\end{aligned}$$

$$\begin{aligned}
& + \left[-\frac{12x_2}{x_1^2} - \frac{6x_3}{x_1^2} + \frac{18(x_2 - x_3)^2}{x_1^3} \right] \frac{\partial \Phi}{\partial x_1}(x_1, x_2, x_3) \\
& + \left[\frac{12x_2}{x_1^3} + \frac{6x_3}{x_1^3} - \frac{18(x_2 - x_3)^2}{x_1^4} \right] (\Phi(x_1, x_2, x_3) - \varphi_0(x_2, x_3)) \\
& + \frac{2x_3^2(x_2 - x_3)}{x_1^2} \left[\frac{\partial^3 \Phi}{\partial x_3^3}(x_1, x_2, x_3) - \frac{\partial^3 \varphi_0}{\partial x_3^3}(x_2, x_3) \right] \\
& + \left[\frac{3x_\alpha x_\beta}{x_1^2} - \frac{9x_\beta^2}{x_1^2} \right] \left[\frac{\partial^2 \Phi}{\partial x_3^2}(x_1, x_2, x_3) - \frac{\partial^2 \varphi_0}{\partial x_3^2}(x_2, x_3) \right] \\
& - \left[\frac{3x_\alpha}{x_1^2} + \frac{9x_\beta}{x_1^2} + \frac{18x_3(x_2 - x_3)}{x_1^3} \right] \left[\frac{\partial \Phi}{\partial x_3}(x_1, x_2, x_3) \right. \\
& \left. - \frac{\partial \varphi_0}{\partial x_3}(x_2, x_3) \right] - 6x_3(x_2 - x_3 + x_1) \frac{\partial^4 \Phi}{\partial x_1^3 \partial x_3}(x_1, x_2, x_3) \\
& + 6x_3(x_2 + x_3 - x_1) \frac{\partial^4 \Phi}{\partial x_1^2 \partial x_3^2}(x_1, x_2, x_3) \\
& - 2x_3^2 \left(1 + \frac{x_2 - x_3}{x_1} \right) \frac{\partial^4 \Phi}{\partial x_1 \partial x_3^3}(x_1, x_2, x_3) \\
& + \left[3x_1 - 3x_2 - 18x_3 - \frac{9x_3(x_2 - x_3)}{x_1} \right] \frac{\partial^3 \Phi}{\partial x_1^2 \partial x_3}(x_1, x_2, x_3) \\
& + \left[-21x_3 - \frac{3x_2 x_3}{x_1} + \frac{9x_3^2}{x_1} \right] \frac{\partial^3 \Phi}{\partial x_1 \partial x_3^2}(x_1, x_2, x_3) \\
& - \left[6 - \frac{12x_2}{x_1} + \frac{6x_3}{x_1} - \frac{18x_3(x_2 - x_3)}{x_1^2} \right] \frac{\partial^2 \Phi}{\partial x_1 \partial x_3}(x_1, x_2, x_3) , \\
T_{11}(x_1, x_2, x_3) & = \frac{2 \ln x_3}{x_1} - \frac{4(x_2 - x_3)}{x_1^2} - \frac{4(x_2 \ln x_2 - x_3 \ln x_3)}{x_1^2} \\
& - \frac{4(x_2 - x_3)}{x_1^3} (\Phi(x_1, x_2, x_3) - \varphi_0(x_2, x_3)) + \frac{4(x_2 - x_3)}{x_1^2} \frac{\partial \Phi}{\partial x_1}(x_1, x_2, x_3) \\
& - \left(1 + \frac{2(x_2 - x_3)}{x_1} \right) \frac{\partial^2 \Phi}{\partial x_1^2}(x_1, x_2, x_3) - \frac{2x_3}{x_1^2} \left(\frac{\partial \Phi}{\partial x_3}(x_1, x_2, x_3) \right. \\
& \left. - \frac{\partial \varphi_0}{\partial x_3}(x_2, x_3) \right) + \frac{x_3(x_2 - x_3)}{x_1^2} \left(\frac{\partial^2 \Phi}{\partial x_3^2}(x_1, x_2, x_3) - \frac{\partial^2 \varphi_0}{\partial x_3^2}(x_2, x_3) \right) \\
& - 2 \frac{\partial^2 \Phi}{\partial x_1 \partial x_3}(x_1, x_2, x_3) - x_3 \left(1 + \frac{x_2 - x_3}{x_1} \right) \frac{\partial^3 \Phi}{\partial x_1 \partial x_3^2}(x_1, x_2, x_3) \\
& + (x_2 + x_3 - x_1) \frac{\partial^3 \Phi}{\partial x_1^2 \partial x_3}(x_1, x_2, x_3) , \\
T_{12}(x_1, x_2, x_3) & = -\frac{52}{x_1^2} + \frac{4}{x_1 x_3} + \frac{20}{x_1^2} \ln x_1 - \frac{18 \ln x_3}{x_1^2} - \frac{20}{x_1^2} \varrho_{1,1}(x_2, x_3) \\
& - \frac{12}{x_1^3} (\Phi(x_1, x_2, x_3) - \varphi_0(x_2, x_3)) + \frac{12}{x_1^2} \frac{\partial \Phi}{\partial x_1}(x_1, x_2, x_3)
\end{aligned}$$

$$\begin{aligned}
& -\frac{6}{x_1} \frac{\partial^2 \Phi}{\partial x_1^2}(x_1, x_2, x_3) - \left(17 \frac{\partial^3 \Phi}{\partial x_1^3} + 2x_1 \frac{\partial^4 \Phi}{\partial x_1^4}\right)(x_1, x_2, x_3) \\
& + \frac{6}{x_1^2} \left(1 + \frac{2(x_2 - x_3)}{x_1}\right) \left(\frac{\partial \Phi}{\partial x_3}(x_1, x_2, x_3) - \frac{\partial \varphi_0}{\partial x_3}(x_2, x_3)\right) \\
& - \frac{3(x_2 - 2x_3)}{x_1^2} \left(\frac{\partial^2 \Phi}{\partial x_3^2}(x_1, x_2, x_3) - \frac{\partial^2 \varphi_0}{\partial x_3^2}(x_2, x_3)\right) \\
& - \frac{x_3(x_2 - x_3)}{x_1^2} \left(\frac{\partial^3 \Phi}{\partial x_3^3}(x_1, x_2, x_3) - \frac{\partial^3 \varphi_0}{\partial x_3^3}(x_2, x_3)\right) \\
& - x_3 \left(1 - \frac{x_2 - x_3}{x_1}\right) \frac{\partial^4 \Phi}{\partial x_1 \partial x_3^3}(x_1, x_2, x_3) \\
& - \frac{6}{x_1} \left(1 + \frac{2(x_2 - x_3)}{x_1}\right) \frac{\partial^2 \Phi}{\partial x_1 \partial x_3}(x_1, x_2, x_3) \\
& - \left[3 \left(1 - \frac{x_2 - 2x_3}{x_1}\right) \frac{\partial^3 \Phi}{\partial x_1 \partial x_3^2} + 6 \left(2 - \frac{x_2 - x_3}{x_1}\right) \frac{\partial^3 \Phi}{\partial x_1^2 \partial x_3}\right](x_1, x_2, x_3) \\
& + 3(x_2 - x_3 - x_1) \frac{\partial^4 \Phi}{\partial x_1^3 \partial x_3}(x_1, x_2, x_3) - 6 \frac{\partial^4 \Phi}{\partial x_1^2 \partial x_3^2}(x_1, x_2, x_3), \\
T_{13}(x_1, x_2, x_3) &= \frac{1}{x_1 x_3} + \frac{2}{x_1^2} \left(\frac{\partial \Phi}{\partial x_3}(x_1, x_2, x_3) - \frac{\partial \varphi_0}{\partial x_3}(x_2, x_3)\right) - \frac{2}{x_1} \frac{\partial^2 \Phi}{\partial x_1 \partial x_3}(x_1, x_2, x_3) \\
& - \frac{x_2 - x_3}{x_1^2} \left(\frac{\partial^2 \Phi}{\partial x_3^2}(x_1, x_2, x_3) - \frac{\partial^2 \varphi_0}{\partial x_3^2}(x_2, x_3)\right) \\
& - \left(1 - \frac{x_2 - x_3}{x_1}\right) \frac{\partial^3 \Phi}{\partial x_1 \partial x_3^2}(x_1, x_2, x_3) - 2 \frac{\partial^3 \Phi}{\partial x_1^2 \partial x_3}(x_1, x_2, x_3), \\
F_1(x_1, x_2, x_3, x_4) &= \frac{1}{x_1 x_2} \frac{\partial}{\partial x_4} \left((x_3 - x_4) \varphi_0\right)(x_3, x_4) \\
& + \frac{1}{x_1 - x_2} \left\{ \frac{\partial}{\partial x_4} \left[\left(1 + \frac{x_3 - x_4}{x_1}\right) \Phi\right](x_1, x_3, x_4) \right. \\
& \left. - \frac{\partial}{\partial x_4} \left[\left(1 + \frac{x_3 - x_4}{x_2}\right) \Phi\right](x_2, x_3, x_4) \right\}, \\
F_2(x_1, x_2, x_3, x_4) &= -\frac{1}{x_1 x_2} \frac{\partial}{\partial x_4} \left((x_3 - x_4) \varphi_0\right)(x_3, x_4) \\
& + \frac{1}{x_1 - x_2} \left\{ \frac{\partial}{\partial x_4} \left[\left(1 - \frac{x_3 - x_4}{x_1}\right) \Phi\right](x_1, x_3, x_4) \right. \\
& \left. - \frac{\partial}{\partial x_4} \left[\left(1 - \frac{x_3 - x_4}{x_2}\right) \Phi\right](x_2, x_3, x_4) \right\}, \\
F_3(x_1, x_2, x_3, x_4) &= 2(\ln x_4 - 1) \varrho_{0,1}(x_1, x_2) - \frac{6(x_3 - x_4)}{x_1 x_2} - \frac{6(x_3 \ln x_3 - x_4 \ln x_4)}{x_1 x_2} \\
& + \frac{x_1 x_2 + 2(x_1 + x_2)(x_3 - x_4)}{x_1^2 x_2^2} \varphi_0(x_3, x_4) - \frac{x_3 - 3x_4}{x_1 x_2} \frac{\partial \varphi_0}{\partial x_4}(x_3, x_4)
\end{aligned}$$

$$\begin{aligned}
& -\frac{x_4(x_3-x_4)}{x_1x_2}\frac{\partial^2\varphi_0}{\partial x_4^2}(x_3,x_4) - \left(\frac{\partial}{\partial x_4} + x_4\frac{\partial^2}{\partial x_4^2}\right)\Omega_0(x_1,x_2;x_3,x_4) \\
& + \left(1 - (x_3 - 3x_4)\frac{\partial}{\partial x_4} - x_4(x_3 - x_4)\frac{\partial^2}{\partial x_4^2}\right)\Omega_{-1}(x_1,x_2;x_3,x_4) \\
& - \left(\frac{\partial}{\partial x_1} + \frac{\partial}{\partial x_2}\right)^2 \left[\Omega_1(x_1,x_2;x_3,x_4) + (x_3 - x_4)\Omega_0(x_1,x_2;x_3,x_4)\right] \\
& - 2\left(\frac{\partial}{\partial x_1} + \frac{\partial}{\partial x_2}\right) \left[\frac{\partial\Omega_1}{\partial x_4}(x_1,x_2;x_3,x_4) - (x_3 + x_4)\frac{\partial\Omega_0}{\partial x_4}(x_1,x_2;x_3,x_4)\right] \\
& - 2(x_3 - x_4)\left(\frac{\partial}{\partial x_1} + \frac{\partial}{\partial x_2}\right)\Omega_{-1}(x_1,x_2;x_3,x_4), \\
F_4(x_1,x_2,x_3,x_4) &= 2(\ln x_4 - 1)\varrho_{0,1}(x_1,x_2) - \frac{6(x_3 - x_4)}{x_1x_2} - \frac{6(x_3 \ln x_3 - x_4 \ln x_4)}{x_1x_2} \\
& - \frac{x_1x_2 - 2(x_1 + x_2)(x_3 - x_4)}{x_1^2x_2^2}\varphi_0(x_3,x_4) + \frac{x_3 + x_4}{x_1x_2}\frac{\partial\varphi_0}{\partial x_4}(x_3,x_4) \\
& - \frac{x_4(x_3 - x_4)}{x_1x_2}\frac{\partial^2\varphi_0}{\partial x_4^2}(x_3,x_4) + \left(-\frac{\partial}{\partial x_4} + x_4\frac{\partial^2}{\partial x_4^2}\right)\Omega_0(x_1,x_2;x_3,x_4) \\
& + \left(-1 + (x_3 + x_4)\frac{\partial}{\partial x_4} - x_4(x_3 - x_4)\frac{\partial^2}{\partial x_4^2}\right)\Omega_{-1}(x_1,x_2;x_3,x_4) \\
& + \left(\frac{\partial}{\partial x_1} + \frac{\partial}{\partial x_2}\right)^2 \left[\Omega_1(x_1,x_2;x_3,x_4) - (x_3 - x_4)\Omega_0(x_1,x_2;x_3,x_4)\right] \\
& - 2\left(\frac{\partial}{\partial x_1} + \frac{\partial}{\partial x_2}\right) \left[\Omega_0(x_1,x_2;x_3,x_4) - 2x_4\frac{\partial\Omega_0}{\partial x_4}(x_1,x_2;x_3,x_4)\right] \\
& - 2(x_3 - x_4)\left(\frac{\partial}{\partial x_1} + \frac{\partial}{\partial x_2}\right)\Omega_{-1}(x_1,x_2;x_3,x_4), \\
F_5(x_1,x_2,x_3,x_4) &= -2(2 + \ln x_4)\varrho_{0,1}(x_1,x_2) + \frac{1}{x_1x_2}\varphi_0(x_3,x_4) \\
& - \frac{x_3 - x_4}{x_1x_2}\frac{\partial\varphi_0}{\partial x_4}(x_3,x_4) - \frac{\partial\Omega_0}{\partial x_4}(x_1,x_2;x_3,x_4) \\
& + \left(1 - (x_3 - x_4)\frac{\partial}{\partial x_4}\right)\Omega_{-1}(x_1,x_2;x_3,x_4), \\
F_6(x_1,x_2,x_3,x_4) &= 2(2 + \ln x_4)\varrho_{0,1}(x_1,x_2) - \frac{1}{x_1x_2}\varphi_0(x_3,x_4) \\
& + \frac{x_3 - x_4}{x_1x_2}\frac{\partial\varphi_0}{\partial x_4}(x_3,x_4) - \frac{\partial\Omega_0}{\partial x_4}(x_1,x_2;x_3,x_4) \\
& - \left(1 - (x_3 - x_4)\frac{\partial}{\partial x_4}\right)\Omega_{-1}(x_1,x_2;x_3,x_4). \tag{A1}
\end{aligned}$$

The concrete expression of $\Phi(x, y, z)$ can be found in [16, 27]. In the limit $z \ll x, y$, we can expand $\Phi(x, y, z)$ according z as

$$\Phi(x, y, z) = \varphi_0(x, y) + z\varphi_1(x, y) + \frac{z^2}{2!}\varphi_2(x, y) + \frac{z^3}{3!}\varphi_3(x, y) + \frac{z^4}{4!}\varphi_4(x, y)$$

$$\begin{aligned}
& +2z(\ln z - 1)\left(1 + \varrho_{1,1}(x, y)\right) \\
& -2z^2\left(\frac{\ln z}{2!} - \frac{3}{4}\right)\left(\frac{x+y}{(x-y)^2} + \frac{2xy}{(x-y)^3} \ln \frac{y}{x}\right) \\
& -\frac{2z^3}{(x-y)^2}\left(\frac{\ln z}{3!} - \frac{11}{36}\right)\left(1 + \frac{12xy}{(x-y)^2} + \frac{6xy(x+y)}{(x-y)^3} \ln \frac{y}{x}\right) \\
& -2z^4\left(\frac{\ln z}{4!} - \frac{25}{288}\right)\left(\frac{2x^3 + 58x^2y + 58xy^2 + 2y^3}{(x-y)^6}\right) \\
& +\frac{24xy(x^2 + 3xy + y^2)}{(x-y)^7} \ln \frac{y}{x} + \dots
\end{aligned} \tag{A2}$$

with

$$\varphi_0(x, y) = \begin{cases} (x+y) \ln x \ln y + (x-y)\Theta(x, y), & x > y; \\ 2x \ln^2 x, & x = y; \\ (x+y) \ln x \ln y + (y-x)\Theta(y, x), & x < y. \end{cases} \tag{A3}$$

$$\varphi_1(x, y) = \begin{cases} -\ln x \ln y - \frac{x+y}{x-y}\Theta(x, y), & x > y; \\ 4 - 2 \ln x - \ln^2 x, & x = y; \\ -\ln x \ln y - \frac{x+y}{y-x}\Theta(y, x), & x < y. \end{cases} \tag{A4}$$

$$\varphi_2(x, y) = \begin{cases} \frac{(2x^2+6xy) \ln x - (6xy+2y^2) \ln y}{(x-y)^3} - \frac{4xy}{(x-y)^3}\Theta(x, y), & x > y; \\ -\frac{5}{9x} + \frac{2}{3x} \ln x, & x = y; \\ \frac{(2x^2+6xy) \ln x - (6xy+2y^2) \ln y}{(x-y)^3} - \frac{4xy}{(y-x)^3}\Theta(y, x), & x < y. \end{cases} \tag{A5}$$

$$\varphi_3(x, y) = \begin{cases} -\frac{12xy(x+y)}{(x-y)^5}\Theta(x, y) - \frac{2(x^2+xy+y^2)}{(x-y)^4} \\ + \frac{2(x^3+14x^2y+11xy^2) \ln x - 2(y^3+14xy^2+11x^2y) \ln y}{(x-y)^5}, & x > y; \\ -\frac{53}{150x^2} + \frac{1}{5x^2} \ln x, & x = y; \\ -\frac{12xy(x+y)}{(y-x)^5}\Theta(y, x) - \frac{2(x^2+xy+y^2)}{(x-y)^4} \\ + \frac{2(x^3+14x^2y+11xy^2) \ln x - 2(y^3+14xy^2+11x^2y) \ln y}{(x-y)^5}, & x < y. \end{cases} \tag{A6}$$

$$\varphi_4(x, y) = \begin{cases} -\frac{48xy(x^2+3xy+y^2)}{(x-y)^7}\Theta(x, y) - \frac{2(3x^3+61x^2y+61xy^2+3y^3)}{(x-y)^6} \\ + \frac{4(x^4+3x^3y-45x^2y^2-25xy^3) \ln x - 4(y^4+3y^3x-45x^2y^2-25yx^3) \ln y}{(x-y)^7}, & x > y; \\ -\frac{598}{2205x^3} + \frac{1}{210x^3} \ln x, & x = y; \\ -\frac{48xy(x^2+3xy+y^2)}{(x-y)^7}\Theta(y, x) - \frac{2(3x^3+61x^2y+61xy^2+3y^3)}{(x-y)^6} \\ + \frac{4(x^4+3x^3y-45x^2y^2-25xy^3) \ln x - 4(y^4+3y^3x-45x^2y^2-25yx^3) \ln y}{(x-y)^7}, & x < y. \end{cases} \tag{A7}$$

Here, the function $\Theta(x, y)$ is defined as

$$\Theta(x, y) = \ln x \ln \frac{y}{x} - 2 \ln(x - y) \ln \frac{y}{x} - 2Li_2\left(\frac{y}{x}\right) + \frac{\pi^2}{3}. \quad (\text{A8})$$

- [1] [The Muon $g - 2$ Collaboration], Phys. Rev. Lett. **92**(2004)161802.
- [2] J. P. Miller, E. de Rafael and B. L. Roberts, *Muon ($g-2$): experiment and theory*, Rep. Prog. Phys. **70**(2007)795; F. Jegerlehner, Acta Phys. Polon. B **38**(2007)3021.
- [3] M. Davier, S. Eidelman, A. Hocker and Z. Zhang, Eur. Phys. J. C **31**(2003)503.
- [4] K. Hagiwara, A. Martin, D. Normura and T. Teubner, Phys. Lett. B **557**(2003)69.
- [5] S. Ghozzi, F. Jegerlehner, Phys. Lett. B **583**(2004)222; M. Passera, J. Phys. G **31**(2005)R75; Nucl. Phys. Proc. Suppl. **155**(2006)365; M. Passera, *The calculation of the muon $g-2$ and $\Delta(\alpha(M(Z)^2))$* , PoS HEP2005, (2006)305.
- [6] A. Czarnecki and W. Marciano, Phys. Rev. D **64**(2001)013014; M. Knecht, Lect. Notes. Phys. **629**(2004)37.
- [7] N. Arkani-Hamed and S. Dimopoulos, JHEP **073**(2005)0506.
- [8] N. Arkani-Hamed et al., Nucl. Phys. B **709**(2005)3.
- [9] A. Czarnecki, B. Krause and W. J. Marciano, Phys. Rev. D **52**(1995)2619; Phys. Rev. Lett. **76**(1996)3267; T. Kukhto, E. Kuraev, A. Schiller and Z. Silagadze, Nucl. Phys. B **371**(1992)567.
- [10] S. Heinemeyer, D. Stöckinger and G. Weiglein, Nucl. Phys. B **690**(2004)62.
- [11] S. Heinemeyer, D. Stöckinger and G. Weiglein, Nucl. Phys. B **699**(2004)103.
- [12] C. Chen, C. Geng, Phys. Lett. B **511**(2001)77; A. Arhrib and S. Baek, Phys. Rev. D **65**(2002)075002.
- [13] D. Chang, W. Chang, and W. Keung, Phys. Rev. D **71**(2005)076006.
- [14] G. Giudice, A. Romanino, Phys. Lett. B **634**(2005)69.
- [15] T.-F. Feng, Phys. Rev. D **70**(2004)096012.
- [16] T.-F. Feng, X.-Q. Li, J. Maalampi, X.-M. Zhang, Phys. Rev. D **71**(2005)056005.

- [17] T.-F. Feng, T. Huang, X.-Q. Li, X.-M. Zhang, S.-M. Zhao, Phys. Rev. D **68**(2003)016004; T.-F. Feng, X.-Q. Li, L. Lin, J. Maalampi, and H.-S. Song, Phys. Rev. D **73**(2006)116001.
- [18] M. Bohm, H. Spiesberger, W. Hollik, Fortsch. Phys. **34**(1986)687; A. Denner, *ibid.* **41**(1993)307.
- [19] L. F. Abbott, Nucl. Phys. B **185**(1981)189; M. B. Gavela, G. Girardi, C. Malleville, and P. Sorba, Nucl. Phys. B **193**(1981)257; N. G. Deshpande, M. Nazerimonfared, Nucl. Phys. B **213**(1983)390.
- [20] Y.K. Semertzidis et al., *Sensitive search for a permanent muon electric dipole moment*, hep-ph/0012087.
- [21] B. C. Regan, E. D. Commins, C. J. Schmidt and D. DeMille, Phys. Rev. Lett. **88**(2002)071805.
- [22] D. Kawell, F. Bay, S. Bickman, Y. Jiang and D. Demille, AIP Conf. Proc. **698**(2004)192.
- [23] S. M. Barr and A. Zee, Phys. Rev. Lett. **65**(1990)21.
- [24] D. Chang, W.-Y. Keung, and A. Pilaftsis, Phys. Rev. Lett. **82**(1999)900; **83**(1999)3972(E); A. Pilaftsis, Phys. Lett. B **471**(1999)174; D. Chang, W.-F. Chang, and W.-Y. Keung, *ibid.* **478**(2000)239; A. Pilaftsis, Nucl. Phys. B **644**(2002)263.
- [25] M. Dress, *Some comments on split supersymmetry*, hep-ph/0501106.
- [26] A. Pilaftsis, Phys. Rev. D **58**(1998)096010; Phys. Lett. B **435**(1998)88; A. Pilaftsis, C. E. M. Wagner, Nucl. Phys. B **533**(1999)3; M. Carena, J. Ellis, A. Pilaftsis, C. E. M. Wagner, *ibid.* **586**(2000)92; *ibid.* **625**(2002)345.
- [27] A. I. Davydychev and J. B. Tausk, Nucl. Phys. B. **397**, 123(1993).